Award Number: W81XWH-11-1-0499

TITLE: Deciphering the Translational Determinants of Prostate Cancer Initiation and Progression

PRINCIPAL INVESTIGATOR: Andrew C. Hsieh

CONTRACTING ORGANIZATION: Unversity of California, San Francisco
San Francisco, CA 94158

REPORT DATE: July 2012

TYPE OF REPORT: Annual Summary

PREPARED FOR: U.S. Army Medical Research and Materiel Command
Fort Detrick, Maryland 21702-5012

DISTRIBUTION STATEMENT: Approved for Public Release;
Distribution Unlimited

REPORT DOCUMENTATION PAGE

Form Approved
OMB No. 0704-0188

1. REPORT DATE	2. REPORT TYPE	3. DATES COVERED
1Jul 2012	Annual Summary	1 Jul 2011 - 30 Jun 2012

4. TITLE AND SUBTITLE

Deciphering the Translational Determinants of Prostate Cancer Initiation and Progression

5a. CONTRACT NUMBER

5b. GRANT NUMBER
W81XWH-11-1-0499

5c. PROGRAM ELEMENT NUMBER

6. AUTHOR(S)
Andrew C. Hsieh

E-Mail: Andrew.hsieh@ucsf.edu

5d. PROJECT NUMBER

5e. TASK NUMBER

5f. WORK UNIT NUMBER

7. PERFORMING ORGANIZATION
Unversity of California, San Francisco
San Francisco, CA 94158

8. PERFORMING ORGANIZATION REPORT NUMBER

9. SPONSORING / MONITORING AGENCY NAME(S) AND ADDRESS(ES)
U.S. Army Medical Research and Materiel Command
Fort Detrick, Maryland 21702-5012

10. SPONSOR/MONITOR'S ACRONYM(S)

11. SPONSOR/MONITOR'S REPORT NUMBER(S)

12. DISTRIBUTION / AVAILABILITY STATEMENT
Approved for Public Release; Distribution Unlimited

13. SUPPLEMENTARY NOTES

14. ABSTRACT

My work is focused on determining the molecular mechanism by which aberrant translational control downstream oncogenic PI3K-AKT-mTOR signaling causes and drives prostate cancer progression. The goal of this work is to provide the mechanistic rationale for using novel second-generation mTOR inhibitors in the clinic for the alleviation of human suffering and death from mTOR driven malignancies.

15. SUBJECT TERMS

16. SECURITY CLASSIFICATION OF:			17. LIMITATION OF ABSTRACT	18. NUMBER OF PAGES	19a. NAME OF RESPONSIBLE PERSON
a. REPORT	b. ABSTRACT	c. THIS PAGE			USAMRMC
U	U	U	UU	27	19b. TELEPHONE NUMBER *(include area code)*

Table of Contents

	Page
Introduction……..…….	**4**
Body…….	**5**
Key Research Accomplishments……..	**7**
Reportable Outcomes……	**8**
Conclusion……	**8**
References……	**8**
Appendices……	**10**

Introduction

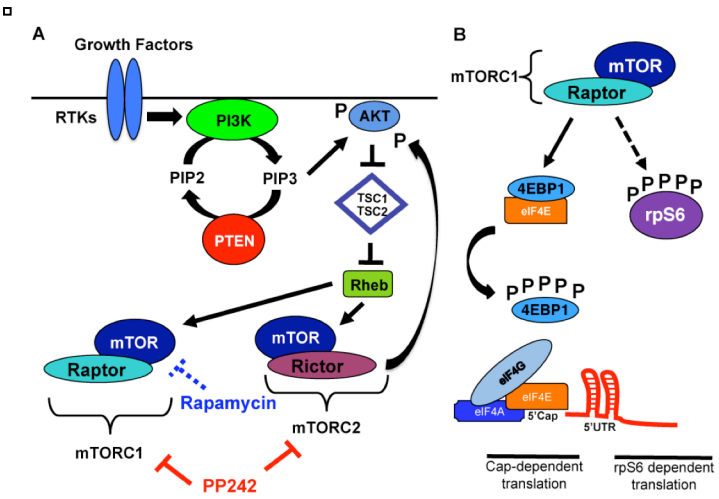

Figure 1. Simplified illustration of the PI3K signal transduction pathway. A. PI3K activation via upstream receptors leads to AKT activation, which subsequently activates mTOR, leading to translational initiation. mTOR co-complexes with either Raptor or Rictor to form two functionally distinct kinases (mTORC1 and mTORC2 respectively). Rapamycin only partially inhibits mTORC1 while PP242 inhibits both mTORC1 and mTORC2. **B.** The specific function of rpS6 is still under investigation. However, 4EBP1 is the tumor suppressor which when hypophosphorylated negatively regulates eIF4E. mTOR-mediated hyperphosphorylation of 4EBP1 leads to dissociation from eIF4E and recruitment of the translational initiation complex (eIF4F – composed of eIF4G, eIF4A (helicase) and eIF4E) to the 5' end of mRNAs.

Despite a wealth of preclinical and clinical data supporting hyperactivation of the mTOR signaling pathway in prostate cancer, allosteric mTOR inhibitors such as rapamycin have demonstrated limited clinical efficacy in prostate cancer[1-6]. We have demonstrated that the inefficacy of allosteric mTOR inhibitors is secondary to incomplete inhibition of the major translational regulator eIF4E binding protein 1 (4EBP1)[7]. 4EBP1 is a known binding partner and inhibitor of the oncogene eIF4E, which is a key rate-limiting initiation factor for cap-dependent translation (the major form of translation in eukaryotes). Phosphorylation of 4EBP1 by mTORC1 leads to its dissociation from eIF4E and allows eIF4E to initiate cap-dependent translation (Fig. 1)[8,9]. As such, the PI3K-AKT-mTOR pathway directly impinges on translational control by regulating the activity of the initiation factor eIF4E, and thereby increases the formation of active initiation complexes responsible for recruiting ribosomes to mRNAs. We hypothesize that inactivation of 4EBP1 by mTOR hyperphosphorylation may represent a major step in PI3K-AKT-mTOR mediated prostate cancer and may account for the poor clinical response to rapalogs. Furthermore, complete inactivation of the mTOR kinase represents a significant therapeutic opportunity towards the treatment of advanced prostate cancer given the development of new ATP site inhibitors of mTOR. This year has been very productive and we just published our most recent findings in Nature based in part from the hypotheses and experiments proposed in this grant (AOP, February 22, 2012, doi:10.1038/nature10911).

Specific Aims

Specific Aim 1: To exploit and determine the efficacy of a novel competitive active-site mTOR inhibitor on prostate cancer initiation and maintenance.

Specific Aim 2: To genetically validate the role of 4EBP1 or rpS6 as the mTOR target necessary for aberrant control of translation downstream of PI3K-AKT-mTOR signaling.

Specific Aim 3: To determine the translationally regulated mRNA targets inhibited by PP242 responsible for improved inhibition of proliferation and increased apoptosis in prostate cancer.

Body

Ribosome profiling of the prostate cancer genome reveals distinct translationally regulated gene networks. The oncogenic mTOR signaling pathway is a major regulator of translational control through the downstream targets 4EBP1 and p70S6 kinase1/2. However, very little is known about how the aberrant translation of specific downstream mRNA targets control cancer initiation and progression. Furthermore, while it has been clearly shown that networks of mRNAs are hijacked at the transcriptional level downstream multiple oncogenic signaling pathways to drive specific cancer cell traits, it is unknown if similar specialized oncogenic programs exist at the post-transcriptional level. In order to determine the specific translationally controlled mRNA targets downstream of mTOR, we optimized ribosome profiling to quantitatively assess ribosome occupancy genome-wide in PC3 prostate cancer cells. In brief, ribosome-protected mRNA fragments were deep-sequenced to determine the number of ribosomes engaged in translating specific mRNAs. We employed short 3-hour drug treatments, which precede alterations in de novo protein synthesis, to capture direct changes in mTOR-dependent gene expression by ribosome profiling and to minimize compensatory feedback mechanisms. mTOR sensitive genes stratify into unique functional categories that may promote cancer development and progression, including cellular invasion (P-value 0.009), cell proliferation (P-value 0.04), metabolism (P-value 0.0002), and regulators of protein modification (P-value 0.01)(Fig. 2a). The largest fraction of mTOR responsive mRNAs cluster into a node consisting of key components of the translational apparatus: 70 ribosomal proteins, 6 elongation factors, and 4 translation initiation factors (P-value 7.5e-82)(Fig. 2a). Therefore, this class of mTOR responsive mRNAs may represent an important regulon that sustains the elevated protein synthetic capacity of cancer cells.

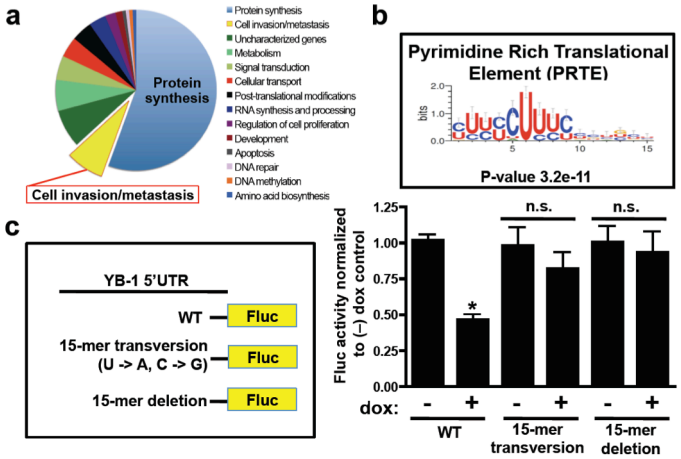

Figure 2. a. Functional classification of translationally regulated mTOR responsive mRNAs. **b.** 15-mer Pyrimidine Rich Translational Element (PRTE) present within the 5' UTRs of 63% of mTOR responsive translationally regulated mRNAs. **c.** Schematic of YB-1 5'UTR cloning (WT, transversion mutant, and deletion mutant of the PRTE (position +20-34, uc001chs.2)) into pGL3-Promoter (Left panel). Firefly luciferase activity in PC3-4EBP1^{M} cells after a 24 hour pre-treatment with 1μg/ml doxycycline followed by transfection of respective 5'UTR constructs (mean ± SEM, n = 9, * P<0.0001, t-test)(Right panel). n.s. – not statistically significant.

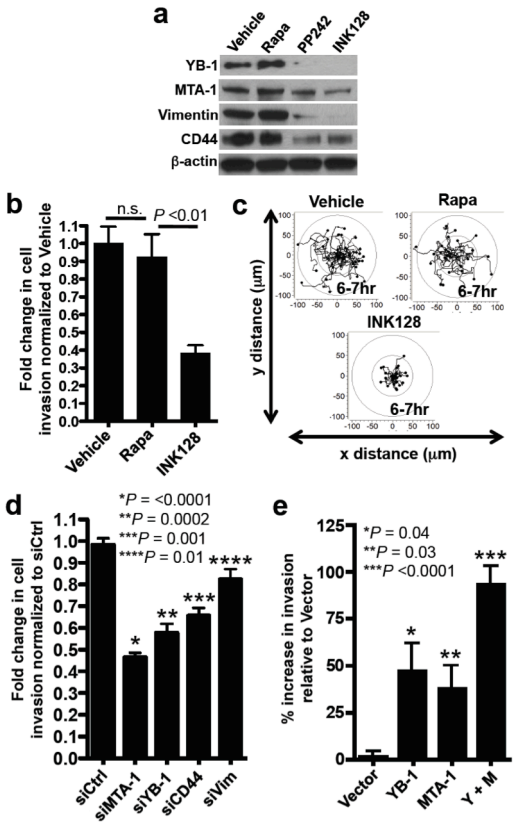

Figure 3. a. Western blot of 4 invasion genes upon drug treatment. **b.** PC3 prostate cancer cell invasion assay after 6-hr drug treatment. **c.** Individual prostate cancer cell migration. **d.** PC3 prostate cancer cell invasion after knockdown of each pro-invasion gene. e. Pro-invasion genes endow untransformed BPH-1 prostate cells with invasion potential.

Discovery of a new cis-regulatory element in mRNAs that are translational targets of mTOR. It has been proposed that mTOR translationally regulated mRNAs may contain long 5' untranslated regions (5'UTRs) with complex RNA secondary structures. Surprisingly, on the contrary, ribosome profiling revealed that mTOR-responsive 5'UTRs possess less complex features (data not shown), providing a unique dataset to investigate the nature of regulatory elements that render mRNAs mTOR-sensitive. It has been previously shown that some mTOR translationally regulated mRNAs, most notably those involved in protein synthesis, possess a 5' terminal oligopyrimidine tract (5'TOP)[10,11] that is regulated by distinct trans-acting factors[12,13]. Of the 144 mTOR sensitive target genes, 67% possess a 5'TOP. However, since the 5'TOP is not present in all mTOR sensitive mRNAs, we next asked whether other 5'UTR consensus sequences may exist. We observed that 63% of mTOR target mRNAs possess what we have termed a Pyrimidine Rich Translational Element (PRTE) within their 5'UTRs

(P-value 3.2e-11). This element, unlike the 5'TOP sequence, consists of an invariant uridine at position 6 flanked by pyrimidines and, importantly, does not reside at position +1 of the 5'UTR (Fig. 2b). Strikingly, 88% of the mTOR-responsive genes possess a PRTE and/or 5'TOP, making the presence of one or both sequences a strong predictor for mTOR sensitivity (data not shown). To test the functional role of the PRTE in mediating translational control, we mutated the PRTE within the 5'UTR of the mTOR responsive gene YB-1, which rendered the YB-1 5'UTR insensitive to inhibition by 4EBP1 (Fig. 3c). These findings highlight a novel *cis*-regulatory element that may modulate translational control of subsets of mRNAs upon mTOR activation.

mTOR governs human prostate cancer migration and invasion through the translational regulation of pro-invasion genes. Strikingly, the second largest node of mTOR translationally regulated genes comprises a novel mRNA signature composed of bona fide cell invasion and metastasis mRNAs and putative regulators of this process (Fig. 3a). This group includes: YB-1 (Y-box binding protein 1), vimentin, MTA-1 (metastasis associated 1), and CD44. YB-1 is a regulator of the post-transcriptional expression of a network of invasion genes[14]. Vimentin, an intermediate filament protein, is highly up-regulated during the epithelial-to-mesenchymal transition (EMT) associated with cellular invasion[15]. MTA-1, a putative chromatin-remodeling gene, is overexpressed in invasive human prostate cancer[16] and has been shown to drive cancer metastasis by promoting neoangiogenesis[17]. CD44 is commonly overexpressed in tumor initiating cells and is implicated in prostate cancer metastasis[18]. Employing either PP242 or its clinical analog INK128, we observed a selective decrease in the expression of YB-1, MTA-1, vimentin, and CD44 at the protein but not transcript level in PC3 cells (Fig. 3a). We next investigated the effects of mTOR ATP site inhibitors on prostate cancer cell migration and invasion. We found that INK128, but not rapamycin, decreases the invasive potential of PC3 prostate cancer cells (Fig. 3b). Furthermore, INK128 inhibits cancer cell migration starting at 6 hours of treatment, precisely correlating with when decreases in the expression of pro-invasion genes are evident, but preceding any changes in the cell cycle or overall global protein synthesis (Figs. 3c, and data not shown). To determine the functional role of each of the genes on prostate cancer cell invasion, we silenced YB-1, MTA-1, CD44, or vimentin gene expression in PC3 cells, and observed a 20-50% reduction in cell invasion (Fig. 3d). These mTOR target mRNAs may be sufficient to endow primary prostate cells with invasive features as overexpression of YB-1 and/or MTA-1 in BPH-1 cells, an untransformed prostate epithelial cell line, increased the invasive capacity of these cells in an additive manner (Fig. 3e). Therefore, translational control of pro-invasion mRNAs by oncogenic mTOR signaling alters the ability of epithelial cells to migrate and invade, a key feature of cancer metastasis.

The 4EBP1/eIF4E axis is necessary for the translational regulation of mTOR sensitive pro-invasion gene expression. We sought to determine the molecular mechanism by which pro-invasion genes are regulated at the translational level and why these mRNAs are sensitive to INK128, but not rapamycin. To this end, we asked if the translational regulators downstream mTORC1, 4EBP1 and/or p70S6K1/2, control the expression of these mTOR sensitive targets. We generated a human prostate cancer cell line that stably expresses a doxycycline inducible dominant negative mutant of 4EBP1 (4EBP1^{M})(Fig. 4a)[19]. This mutant binds to eIF4E, decreasing its hyperactivation without inhibiting general mTORC1 function. Importantly, expression of the 4EBP1^{M} does not alter global protein synthesis (data not shown), likely because endogenous 4EBP1/2s retain their ability to bind to eIF4E[19]. Upon induction of the 4EBP1^{M}, YB-1, vimentin, CD44, and MTA-1 decrease at the protein but not mRNA level, while pharmacological inhibition of p70S6K1/2 with DG-2[20] had no effect (Figs. 4b, c, and data not shown). Next we tested if INK128 decreases expression of the 4 invasion genes through the 4EBP1-eIF4E axis. Strikingly, knockdown of 4EBP1/2 in PC3 cells or employing 4EBP1/2 knock-out MEFs[21] reduced the ability of INK128 to decrease expression of these pro-invasion mRNAs (data not shown). Furthermore, ablation of

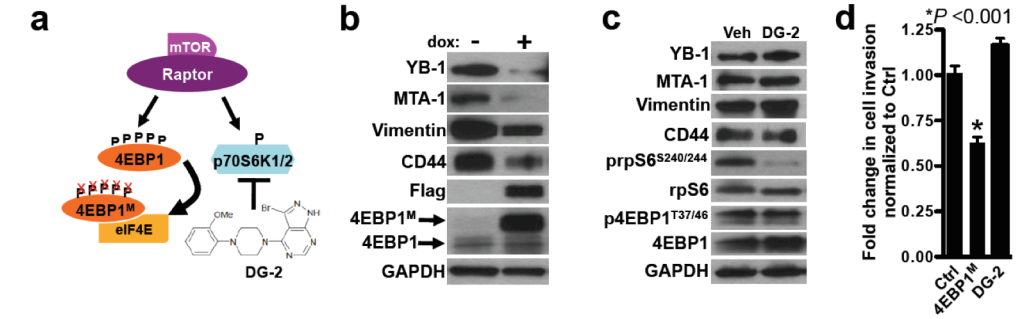

Figure 4. a. Schematic of the pharmacogenetic strategy to inhibit p70S6K1/2 or eIF4E hyperactivation. **b.** Western blot of PC3-4EBP1^{M} cells after 48-hour doxycycline induction of the 4EBP1^{M}. **c.** Western blot of PC3 cells after 48-hour DG-2 treatment. d. Matrigel invasion assay upon 48-hour doxycycline induction of the 4EBP1^{M}, or treatment with DG-2 compared to control (n = 6 per condition, t-test).

mTORC2 activity had no effect on the expression of these mRNAs or responsiveness to INK128 (data not shown). We therefore next determined the effect of the 4EBP1^{M} on human prostate cancer cell invasion. The expression of the 4EBP1^{M} resulted in a significant decrease in prostate cancer cell invasion without affecting the cell cycle, while DG-2 had no effect (Figs. 4d). These findings demonstrate that eIF4E hyperactivation downstream of oncogenic mTOR regulates translational control of the pro-invasion mRNAs and provides an explanation for the selective targeting of this gene signature by mTOR ATP site inhibitors.

ATP site inhibition of mTOR dramatically reduces prostate cancer metastasis *in vivo*. We extended the preclinical trial by examining the effects of INK128 treatment on the pro-invasion gene signature and metastasis, which is incurable and the primary cause of patient mortality. Cell invasion is the critical first step in metastasis, required for systemic dissemination. In PTEN$^{L/L}$ mice after the onset of PIN, a subset of prostate glands exhibit characteristics of luminal epithelial cell invasion by 12 months (Fig. 5a)[22]. After 12 months of age, PTEN$^{L/L}$ mice develop lymph node metastases that maintain strong YB-1 and MTA-1 expression (Fig. 5b). We further extended these findings directly to human prostate cancer patient specimens, observing that YB-1 expression levels increase in a stepwise fashion from normal prostate to CRPC, an advanced form of the disease associated with increased metastatic potential (Fig. 5c). MTA-1 levels exhibit similar increases[16]. In human prostate cancer, high-grade primary tumors that display invasive features are more likely to develop systemic metastasis than low-grade noninvasive tumors[23,24]. Strikingly, treatment with INK128 completely blocked the progression of invasive prostate cancer locally in the prostate gland, and profoundly inhibited the total number and size of distant metastases (Figs. 5d-f). This was associated with a marked decrease in the expression of YB-1, vimentin, CD44, and MTA-1 at the protein but not transcript level in specific epithelial cell types of pre-invasive PIN lesions in PTEN$^{L/L}$ mice (Fig. 5g). Together, these findings reveal an unexpected role for oncogenic mTOR signaling in control of a pro-invasion translation program that, along with the lethal metastatic form of prostate cancer, can be efficiently targeted with clinically relevant mTOR ATP site inhibitors.

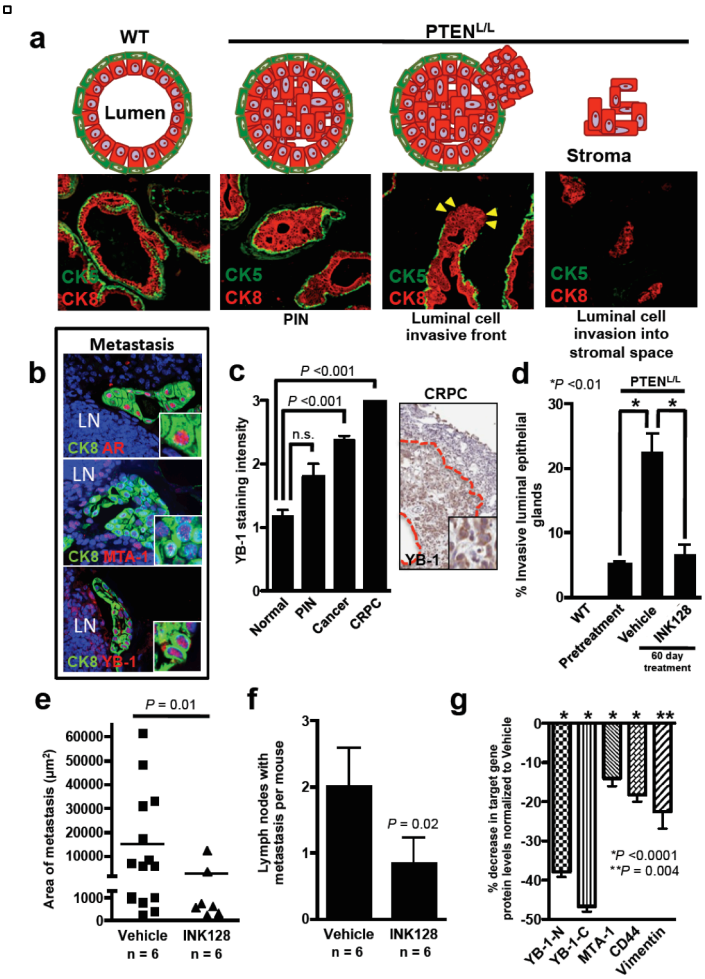

Figure 5. a. Diagram and images of normal prostate gland, pre-invasive PIN and invasive prostate cancer. CK8/CK5 = luminal/basal epithelial cells respectively. Yellow triangles = invasive front. **b.** Immunofluorescent images of 14-month-old PTEN$^{L/L}$ lymph node (LN) metastasis co-stained with CK8/androgen receptor (AR), CK8/YB-1, and CK8/MTA-1**. c.** Human tissue microarray of YB-1 protein levels in normal, PIN, cancer, and CRPC (ANOVA)(left panel). Immunohistochemistry of YB-1 in human CRPC demarcated by the red line (*inset* nuclear and cytoplasmic YB-1)(right panel). **d.** Quantification of invasive prostate glands in WT and PTEN$^{L/L}$ mice before (12 months old) and after (14 months old) 60 days of INK128 treatment (n = 6 mice/arm, ANOVA). **e, f.** Area and number of CK8/AR+ metastasis in draining lymph nodes in 14 month old PTEN$^{L/L}$ mice after 60 days of INK128 treatment (n = 6 mice/arm, t-test). **g.** Percent decrease of YB-1, MTA-1, CD44, or vimentin protein levels (determined by quantitative immunofluorescence) in CK8+ or CK5+ prostate cells (CK8+ only for vimentin) in INK128 treated 14 month old PTEN$^{L/L}$ mice normalized to vehicle treated mice (n = 3 mice/arm, t-test).

Key Research Accomplishments

- First ever ribosome profiling of a human cancer.
- Discovery of translationally regulated gene networks which drive prostate cancer progression.
- Discovery of the PRTE, a new *cis*-regulatory element in the 5' UTRs of mTOR sensitive genes.
- First publication of the chemical structure of INK128.
- ATP site inhibition of the mTOR kinase significantly diminishes the invasive capacity of prostate cancer cells.
- Prostate cancer metastasis is druggable through stringent mTOR inhibition.
- The translational landscape of the cancer genomes represents a new therapeutic target in the fight against advanced prostate cancer.

Reportable Outcomes

Oral presentations:

Hsieh AC. Genome-wide analysis and characterization of translational regulons controlled by mTOR signaling. 2011 EMBO Conference Series on Protein Synthesis and Translational Control. Heidelberg, Germany.

Abstracts:

- **Hsieh AC**, Ruggero D. The translational landscape of mTOR signaling directs cancer initiation and progression. 2012 27th Aspen Cancer Conference, Aspen, CO (Poster).

- **Hsieh AC**, Liu Y, Ingolia NT, Edlind MP, Christensen C, Bok R, Scott K, Feldman ME, Kurhanewicz J, Shokat KM, Weissman JS, Rommel C, Ruggero D. Translational control in prostate cancer. 2011 AACR Special Conference on Targeting PI3K/mTOR Signaling in Cancer, San Francisco, CA (Poster).

- Amin DN, **Hsieh AC,** Sergina N, McMahon M, Ruggero D, Shokat KM, Moasser, MM. mTORC1-driven negative feedback signaling protects HER2-HER3 tumorigenic signaling in breast cancers. 2011 AACR Special Conference on Targeting PI3K/mTOR Signaling in Cancer, San Francisco, CA (Poster).

Peer reviewed publications:

- **Hsieh AC**, Liu Y, Edlind MP, Ingolia, NT, Janes MR, Sher A, Shi EY, Christensen C, Stumpf CR, Bonham MJ, Wang S, Ren P, Martin M, Jessen K, Feldman ME, Weissman JS, Shokat KM, Rommel C, Ruggero D. The translational landscape of oncogenic mTOR signaling controls cancer development and metastasis. **Nature** 485(7396); 2012, 55-61. PMID: 22367541

- Kondrashov N, Pusic A, Stumpf, CR, Shimizu K, **Hsieh AC**, Ishijima J, Kikkawa Y, Shiroishi T, Barna M. Ribosome mediated specificity of Hox mRNA translation and vertebrate tissue patterning. **Cell** 145(3); 2011. PMID: 21529712

- **Hsieh AC**, Truitt ML, Ruggero D. Oncogenic AKTivation of translation as a therapeutic target. **Br J Cancer** 105(3); 2011. PMC3172900 *Invited Review*

Other Funding: June 2012 – Submitted application for K08 to the NIH-NCI

Recognition, Promotions, or Awards: As of July 2011 I have been promoted to Adjunct Instructor in the Department of Medicine, Division of Hematology/Oncology UCSF.

Conclusion

We have generated the first map of the translational landscape of human prostate cancer. Furthermore, we have linked these findings to a robustly druggable target, namely the mTOR kinase and have identified a key role of this oncogenic kinase in prostate cancer progression. In particular, we have delineated a novel mechanism by which the mTOR kinase drives the aberrant expression of critical genes at the translational level to promote prostate cancer invasion and metastasis. Moreover, we show *in vivo* that novel ATP site inhibitors of mTOR, currently in Phase I-II clinical trials in solid tumors, effectively inhibit the expression of these genes resulting in a profound cytotoxic effect, which halts prostate cancer progression. These findings provide the mechanistic rationale for the use of ATP site mTOR inhibitors in advanced prostate cancer. Furthermore, we have identified potential biomarkers for disease progression and the therapeutic response to these novel inhibitors.

References

1 Amato, R. J., Jac, J., Mohammad, T. & Saxena, S. Pilot study of rapamycin in patients with hormone-refractory prostate cancer. *Clinical genitourinary cancer* **6**, 97-102 (2008).

2 George, D. J. *et al. A phase II study of RAD001 in men with hormone-refractory metastatic prostate cancer (HRPC)* (2008).
3 Armstrong, A. J. *et al.* A pharmacodynamic study of rapamycin in men with intermediate- to high-risk localized prostate cancer. *Clin Cancer Res* **16**, 3057-3066, doi:1078-0432.CCR-10-0124 [pii]10.1158/1078-0432.CCR-10-0124.
4 Buckle, G. C. *et al. Phase II trial of RAD001 and Bicalutamide for castration-resistant prostate cancer (CRPC).* (2010).
5 Zhang, W. *et al.* Inhibition of tumor growth progression by antiandrogens and mTOR inhibitor in a Pten-deficient mouse model of prostate cancer. *Cancer research* **69**, 7466-7472, doi:10.1158/0008-5472.CAN-08-4385 (2009).
6 Nardella, C. *et al.* Differential Requirement of mTOR in Postmitotic Tissues and Tumorigenesis. *Science signaling* **2**, ra2, doi:10.1126/scisignal.2000189 (2009).
7 Hsieh, A. C. *et al.* Genetic dissection of the oncogenic mTOR pathway reveals druggable addiction to translational control via 4EBP-eIF4E. *Cancer cell* **17**, 249-261, doi:S1535-6108(10)00039-5 [pii]10.1016/j.ccr.2010.01.021.
8 Gingras, A. C., Kennedy, S. G., O'Leary, M. A., Sonenberg, N. & Hay, N. 4E-BP1, a repressor of mRNA translation, is phosphorylated and inactivated by the Akt(PKB) signaling pathway. *Genes & development* **12**, 502-513 (1998).
9 Gingras, A. C. *et al.* Regulation of 4E-BP1 phosphorylation: a novel two-step mechanism. *Genes & development* **13**, 1422-1437 (1999).
10 Tang, H. *et al.* Amino acid-induced translation of TOP mRNAs is fully dependent on phosphatidylinositol 3-kinase-mediated signaling, is partially inhibited by rapamycin, and is independent of S6K1 and rpS6 phosphorylation. *Mol Cell Biol* **21**, 8671-8683, doi:10.1128/MCB.21.24.8671-8683.2001 (2001).
11 Meyuhas, O. Synthesis of the translational apparatus is regulated at the translational level. *European journal of biochemistry / FEBS* **267**, 6321-6330, doi:ejb1719 [pii] (2000).
12 Crosio, C., Boyl, P. P., Loreni, F., Pierandrei-Amaldi, P. & Amaldi, F. La protein has a positive effect on the translation of TOP mRNAs in vivo. *Nucleic acids research* **28**, 2927-2934 (2000).
13 Orom, U. A., Nielsen, F. C. & Lund, A. H. MicroRNA-10a binds the 5'UTR of ribosomal protein mRNAs and enhances their translation. *Mol Cell* **30**, 460-471, doi:S1097-2765(08)00328-6 [pii]10.1016/j.molcel.2008.05.001 (2008).
14 Evdokimova, V. *et al.* Translational activation of snail1 and other developmentally regulated transcription factors by YB-1 promotes an epithelial-mesenchymal transition. *Cancer cell* **15**, 402-415, doi:S1535-6108(09)00086-5 [pii]10.1016/j.ccr.2009.03.017 (2009).
15 Lahat, G. *et al.* Vimentin is a novel anti-cancer therapeutic target; insights from in vitro and in vivo mice xenograft studies. *PLoS One* **5**, e10105, doi:10.1371/journal.pone.0010105.
16 Hofer, M. D. *et al.* The role of metastasis-associated protein 1 in prostate cancer progression. *Cancer research* **64**, 825-829 (2004).
17 Yoo, Y. G., Kong, G. & Lee, M. O. Metastasis-associated protein 1 enhances stability of hypoxia-inducible factor-1alpha protein by recruiting histone deacetylase 1. *EMBO J* **25**, 1231-1241, doi:7601025 [pii]10.1038/sj.emboj.7601025 (2006).
18 Liu, C. *et al.* The microRNA miR-34a inhibits prostate cancer stem cells and metastasis by directly repressing CD44. *Nature medicine* **17**, 211-215, doi:nm.2284 [pii]10.1038/nm.2284.
19 Hsieh, A. C. *et al.* Genetic Dissection of the Oncogenic mTOR Pathway Reveals Druggable Addiction to Translational Control via 4EBP-eIF4E. *Cancer cell* **17**, 249-261, doi:10.1016/j.ccr.2010.01.021 (2010).
20 Okuzumi, T. *et al.* Inhibitor hijacking of Akt activation. *Nat Chem Biol* **5**, 484-493, doi:nchembio.183 [pii]10.1038/nchembio.183 (2009).
21 Dowling, R. J. *et al.* mTORC1-mediated cell proliferation, but not cell growth, controlled by the 4E-BPs. *Science (New York, N.Y* **328**, 1172-1176, doi:328/5982/1172 [pii]10.1126/science.1187532.
22 Wang, S. *et al.* Prostate-specific deletion of the murine Pten tumor suppressor gene leads to metastatic prostate cancer. *Cancer cell* **4**, 209-221 (2003).
23 Pontes, J. E., Wajsman, Z., Huben, R. P., Wolf, R. M. & Englander, L. S. Prognostic factors in localized prostatic carcinoma. *The Journal of urology* **134**, 1137-1139 (1985).
24 Zhou, P. *et al.* Predictors of prostate cancer-specific mortality after radical prostatectomy or radiation therapy. *J Clin Oncol* **23**, 6992-6998, doi:23/28/6992 [pii]10.1200/JCO.2005.01.2906 (2005).

ARTICLE

doi:10.1038/nature10912

The translational landscape of mTOR signalling steers cancer initiation and metastasis

Andrew C. Hsieh[1,2]*, Yi Liu[3]*, Merritt P. Edlind[1], Nicholas T. Ingolia[4], Matthew R. Janes[3], Annie Sher[1], Evan Y. Shi[1], Craig R. Stumpf[1], Carly Christensen[1], Michael J. Bonham[5], Shunyou Wang[3], Pingda Ren[3], Michael Martin[3], Katti Jessen[3], Morris E. Feldman[6], Jonathan S. Weissman[6], Kevan M. Shokat[6], Christian Rommel[3] & Davide Ruggero[1]

The mammalian target of rapamycin (mTOR) kinase is a master regulator of protein synthesis that couples nutrient sensing to cell growth and cancer. However, the downstream translationally regulated nodes of gene expression that may direct cancer development are poorly characterized. Using ribosome profiling, we uncover specialized translation of the prostate cancer genome by oncogenic mTOR signalling, revealing a remarkably specific repertoire of genes involved in cell proliferation, metabolism and invasion. We extend these findings by functionally characterizing a class of translationally controlled pro-invasion messenger RNAs that we show direct prostate cancer invasion and metastasis downstream of oncogenic mTOR signalling. Furthermore, we develop a clinically relevant ATP site inhibitor of mTOR, INK128, which reprograms this gene expression signature with therapeutic benefit for prostate cancer metastasis, for which there is presently no cure. Together, these findings extend our understanding of how the 'cancerous' translation machinery steers specific cancer cell behaviours, including metastasis, and may be therapeutically targeted.

It is unknown whether specialized networks of translationally controlled mRNAs can direct cancer initiation and progression, thereby mirroring cooperativity that has mainly been observed at the level of transcriptional control. This is an important question, as key oncogenic signalling molecules, such as the mTOR kinase, directly regulate the activity of general translation factors[1,2]. Downstream of the phosphatidylinositol-3-OH kinase (PI(3)K)–AKT signalling pathway, mTOR assembles with either raptor or rictor to form two distinct complexes: mTORC1 and mTORC2 (refs 3, 4). The major regulators of protein synthesis downstream of mTORC1 are 4EBP1 (also called EIF4EBP1) and p70S6K1/2 (refs 1, 2). 4EBP1 negatively regulates eIF4E, a key rate-limiting initiation factor for cap-dependent translation. Phosphorylation of 4EBP1 by mTORC1 leads to its dissociation from eIF4E, allowing translation initiation complex formation at the 5′ end of mRNAs[5]. The mTOR-dependent phosphorylation of p70S6K1/2 also promotes translation initiation as well as elongation[6]. At a genome-wide level, it remains poorly understood whether and how activation of these regulators of protein synthesis may produce specific changes in gene expression networks that direct cancer development. Here we use a powerful new technology known as ribosome profiling to delineate the translational landscape of the cancer genome at a codon-by-codon resolution upon pharmacological inhibition of mTOR[7]. Our findings provide genome-wide characterization of translationally controlled mRNAs downstream of oncogenic mTOR signalling and delineate their functional roles in cancer development. Moreover, we determine the efficacy of a novel clinically relevant mTOR inhibitor that we developed, INK128, which specifically targets this cancer program.

Ribosome profiling of the prostate cancer genome

mTOR is deregulated in nearly 100% of advanced human prostate cancers[8], and genetic findings in mouse models implicate mTOR hyperactivation in prostate cancer initiation[9–11]. Given the critical role for mTOR in prostate cancer, we used PC3 human prostate cancer cells, where mTOR is constitutively hyperactivated, to delineate translationally controlled gene expression networks upon complete or partial mTOR inhibition. We optimized ribosome profiling to assess quantitatively ribosome occupancy genome-wide in cancer cells[7]. In brief, ribosome-protected mRNA fragments were deep-sequenced to determine the number of ribosomes engaged in translating specific mRNAs (Supplementary Fig. 1a and Methods). Treatment of PC3 cells with PP242 (refs 12, 13), an mTOR ATP site inhibitor, significantly inhibits the activity of the three primary downstream mTOR effectors 4EBP1, p70S6K1/2 and AKT. On the contrary, rapamycin, an allosteric mTOR inhibitor, only blocks p70S6K1/2 activity in these cells (Supplementary Fig. 1b). We used short 3-h drug treatments, which precede alterations in *de novo* protein synthesis, to capture direct changes in mTOR-dependent gene expression by ribosome profiling and to minimize compensatory feedback mechanisms (Supplementary Fig. 1c–f).

Ribosome profiling revealed 144 target mRNAs selectively decreased at the translational level upon PP242 treatment ($\log_2 \leq -1.5$ (false discovery rate <0.05)) compared to rapamycin treatment, with limited changes in transcription (Fig. 1a and Supplementary Figs 2a, b and 3–10). The fact that at this time point rapamycin treatment did not markedly affect gene expression is consistent with incomplete allosteric inhibition of mTOR activity (Supplementary Fig. 1b). By

[1]School of Medicine and Department of Urology, Helen Diller Family Comprehensive Cancer Center, University of California, San Francisco, California 94158, USA. [2]Division of Hematology/Oncology and Department of Internal Medicine, University of California, San Francisco, California 94143, USA. [3]Intellikine Inc., La Jolla, California 92037, USA. [4]Carnegie Institution for Science, Baltimore, Maryland 21218, USA. [5]Department of Pathology, University of California, San Francisco, California 94143, USA. [6]Howard Hughes Medical Institute, Department of Cellular and Molecular Pharmacology, University of California, San Francisco, California 94158, USA.
*These authors contributed equally to this work.

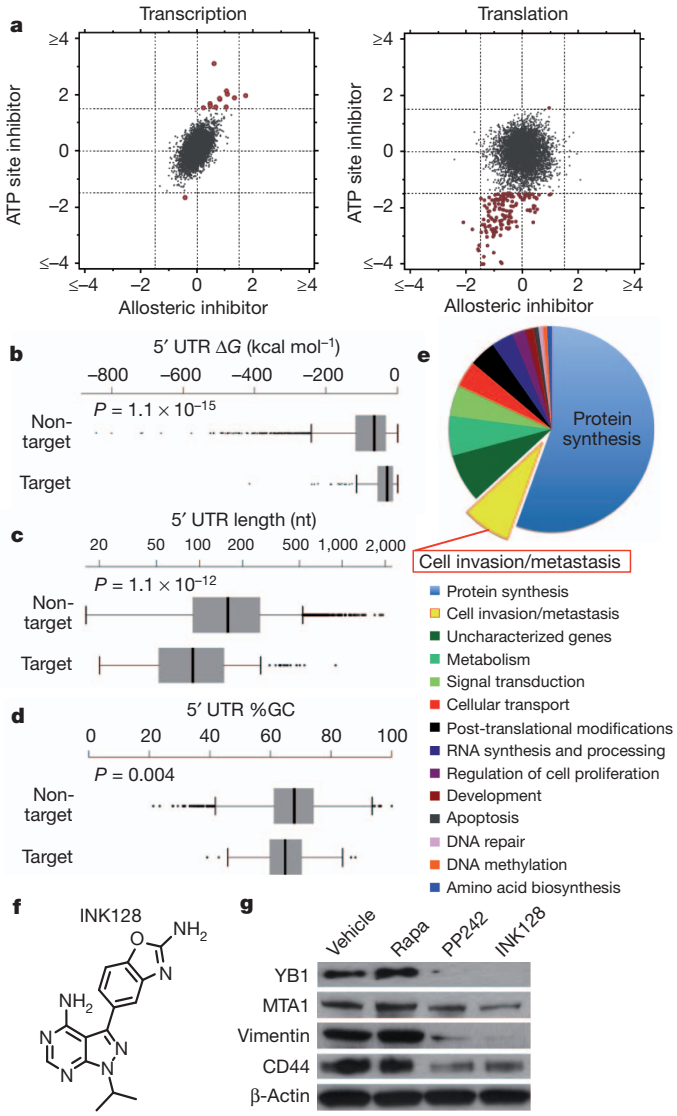

Figure 1 | Ribosome profiling reveals mTOR-dependent specialized translational control of the prostate cancer genome. **a**, Representative comparison of mRNA abundance and translational efficiency after a 3-h treatment with an ATP site inhibitor (PP242) versus an allosteric inhibitor (rapamycin). **b**–**d**, Free energy, length and percentage G+C content of the 5′ UTRs of mTOR target versus non-target mRNAs (error bars indicate range, non-target $n = 5{,}022$, target $n = 144$, two-sided Wilcoxon). **e**, Functional classification of translationally regulated mTOR-responsive mRNAs. **f**, Chemical structure of INK128. **g**, Representative western blot from three independent experiments of mTOR-sensitive invasion genes in PC3 cells after a 48-h drug treatment. Rapa, rapamycin.

monitoring footprints of translating 80S ribosomes, our findings show that the effects of PP242 are largely at the level of translation initiation and not elongation (Supplementary Fig. 3). It has been proposed that mRNAs translationally regulated by mTOR may contain long 5′ untranslated regions (5′ UTRs) with complex RNA secondary structures. On the contrary, ribosome profiling revealed that mTOR-responsive 5′ UTRs possess less complex features (Fig. 1b–d), providing a unique data set to investigate the nature of regulatory elements that render these mRNAs mTOR-sensitive. It has been previously shown that some mTOR translationally regulated mRNAs, most notably those involved in protein synthesis, possess a 5′ terminal oligopyrimidine tract (5′ TOP)[14,15] that is regulated by distinct *trans*-acting factors[16,17]. Of the 144 mTOR-sensitive target genes, 68% possess a 5′ TOP. However, as the 5′ TOP is not present in all mTOR-sensitive mRNAs, we next asked whether other 5′ UTR consensus sequences may exist. Strikingly, 63% of mTOR target mRNAs possess what we have termed a pyrimidine-rich translational element (PRTE) within their 5′ UTRs ($P = 3.2 \times 10^{-11}$). This element, unlike the 5′ TOP sequence, consists of an invariant uridine at position 6 flanked by pyrimidines and, importantly, does not reside at position +1 of the 5′ UTR (Supplementary Figs 2c and 7). We found that 89% of the mTOR-responsive genes possess a PRTE and/or 5′ TOP, making the presence of one or both sequences a strong predictor for mTOR sensitivity (Supplementary Figs 2d and 7). Notably, mRNA isoforms arising from distinct transcription start sites may possess both a 5′ TOP and a PRTE. Moreover, given the significant number of mRNAs that contain both the PRTE and 5′ TOP, a functional interplay may exist between these regulatory elements. Future studies are required to determine the regulatory logic for how these sequences either independently or coordinately confer mTOR responsiveness. Multiple *cis*-acting elements within specific 5′ UTRs could reflect regulation by distinct mTOR effectors. For example, our findings show that the PRTE imparts translational control specificity to 4EBP1 activity (see below).

Surprisingly, mTOR-sensitive genes stratify into unique functional categories that may promote cancer development and progression, including cellular invasion ($P = 0.009$), cell proliferation ($P = 0.04$), metabolism ($P = 0.0002$) and regulators of protein modification ($P = 0.01$) (Fig. 1e). The largest fraction of mTOR-responsive mRNAs cluster into a node consisting of key components of the translational apparatus: 70 ribosomal proteins, 6 elongation factors, and 4 translation initiation factors ($P = 7.5 \times 10^{-82}$) (Fig. 1e and Supplementary Fig. 5). Therefore, this class of mTOR-responsive mRNAs may represent an important regulon that sustains the elevated protein synthetic capacity of cancer cells.

Notably, the second largest node of mTOR translationally regulated genes comprises bona fide cell invasion and metastasis mRNAs and putative regulators of this process (Fig. 1e). This group includes *YB1* (Y-box binding protein 1; also called YBX1), vimentin, *MTA1* (metastasis associated 1) and *CD44* (Supplementary Fig. 11a). YB1

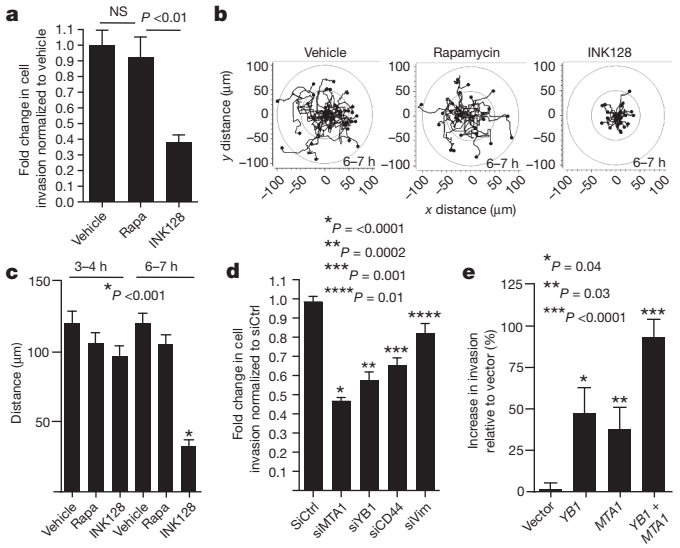

Figure 2 | mTOR promotes prostate cancer cell migration and invasion through a translationally regulated gene signature. **a**, Matrigel invasion assay in PC3 cells: 6-h pre-treatment followed by 6 h of cell invasion ($n = 6$, ANOVA). **b**, **c**, Migration patterns and average distance travelled by GFP-labelled PC3 cells during hours 3–4 and 6–7 of drug treatment ($n = 34$ cells per condition, ANOVA). **d**, Matrigel invasion assay in PC3 cells after 48 h of knockdown of *YB1*, *MTA1*, *CD44*, or vimentin followed by 24 h of cell invasion ($n = 7$, *t*-test). **e**, Matrigel invasion assay in BPH-1 cells after 48 h of overexpression of *YB1* and/or *MTA1*, followed by cell invasion for 24 h ($n = 7$, *t*-test). Rapa, rapamycin. All data represent mean ± s.e.m. NS, not statistically significant.

regulates the post-transcriptional expression of a network of invasion genes[18]. Vimentin, an intermediate filament protein, is highly upregulated during the epithelial-to-mesenchymal transition associated with cellular invasion[19]. MTA1, a putative chromatin-remodelling protein, is overexpressed in invasive human prostate cancer[20] and has been shown to drive cancer metastasis by promoting neoangiogenesis[21]. CD44 is commonly overexpressed in tumour-initiating cells and is implicated in prostate cancer metastasis[22]. Consistent with their status as mTOR sensitive genes, *YB1*, vimentin, *MTA1* and *CD44* all possess a PRTE (Supplementary Fig. 5). Vimentin and *CD44* also possess a 5′ TOP (Supplementary Fig. 7). To test the functional role of the PRTE in mediating translational control, we mutated the PRTE within the 5′ UTR of *YB1*, which rendered the *YB1* 5′ UTR insensitive to inhibition by 4EBP1 (Supplementary Fig. 11b). These findings highlight a novel *cis*-regulatory element that may modulate translational control of subsets of mRNAs upon mTOR activation. Moreover, ribosome profiling reveals unexpected transcript-specific translational control, mediated by oncogenic mTOR signalling, including a distinct set of pro-invasion and metastasis genes.

Translation of pro-invasion mRNAs by mTOR

We next extended the use of the mTOR pharmacological tools used in ribosome profiling towards functional characterization of the newly identified mTOR-sensitive cell invasion gene signature. To this end, we developed a new clinical-grade mTOR ATP site inhibitor, INK128, derived from the PP242 chemical scaffold (Fig. 1f). In brief, a structure-guided optimization of pyrazolopyrimidine derivatives was performed (see INK128 chemical synthesis in Supplementary Information) that improved oral bioavailability while retaining mTOR kinase potency and selectivity. INK128 was selected for clinical studies on the basis of its high potency (1.4 nM inhibition constant (K_i)), selectivity for mTOR, low molecular mass, and favourable pharmaceutical properties (Supplementary Figs 12 and 13).

Using either PP242 or INK128, we observed a selective decrease in the expression of YB1, MTA1, vimentin and CD44 at the protein but not transcript level in PC3 cells starting at 6 h of treatment, which precedes any decrease in *de novo* protein synthesis (Fig. 1g and Supplementary Figs 1c, d, 14 and 15). In contrast, rapamycin treatment did not alter their expression (Fig. 1g and Supplementary Fig. 14a). Similar findings were observed using a broad panel of metastatic cell lines of distinct histological origins (Supplementary Fig. 16). The four-gene invasion signature is positively regulated by mTOR hyperactivation, as silencing PTEN expression increased their protein but not mRNA expression levels (Supplementary Fig. 17). We next investigated the effects of mTOR ATP site inhibitors on prostate cancer cell migration and invasion. We found that INK128, but not rapamycin, decreases the invasive potential of PC3 prostate cancer cells (Fig. 2a). Furthermore, INK128 inhibits cancer cell migration starting at 6 h of treatment, precisely correlating with when decreases in the expression of pro-invasion genes are evident, but preceding any changes in the cell cycle or overall global protein synthesis (Fig. 2b, c, and Supplementary Figs 1c, e, f, 14b and 18).

Among the genes comprising the pro-invasion signature, YB1 has been shown to act directly as a translation factor that controls expression of a larger set of genes involved in breast cancer cell invasion[18]. Notably, YB1 translationally regulated target mRNAs, including *SNAIL1* (also called *SNAI*), *LEF1* and *TWIST1*, decreased at the protein but not transcript level upon *YB1* knockdown in PC3 cells (Supplementary Figs 19 and 20). To determine the functional role of YB1 in prostate cancer cell invasion, we silenced *YB1* gene expression in PC3 cells, and observed a 50% reduction in cell invasion (Fig. 2d). Similarly, knockdown of *MTA1*, *CD44*, or vimentin also inhibited prostate cancer cell invasion (Fig. 2d and Supplementary Fig. 19). These mTOR target mRNAs may be sufficient to endow primary prostate cells with invasive features, as overexpression of *YB1* and/or *MTA1* (Supplementary Fig. 21a) in BPH-1 cells, an untransformed

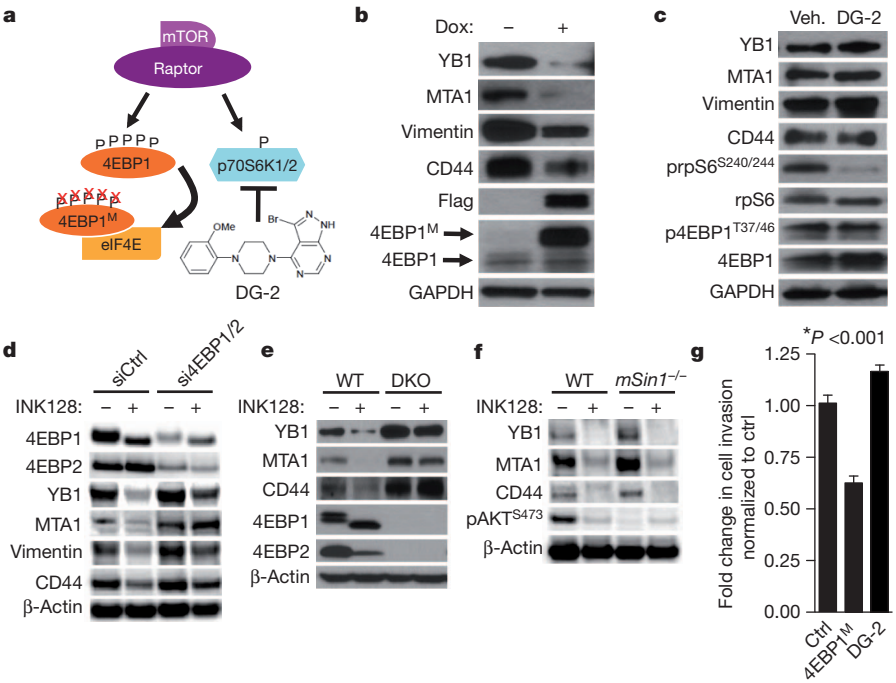

Figure 3 | The 4EBP1–eIF4E axis controls the post-transcriptional expression of mTOR-sensitive invasion genes. **a**, Schematic of the pharmacogenetic strategy to inhibit p70S6K1/2 or eIF4E hyperactivation. **b**, Representative western blot from three independent experiments of PC3 4EBP1^{M} cells after 48-h doxycycline induction of 4EBP1^{M}. **c**, Representative western blot from three independent experiments of PC3 cells after 48-h DG-2 treatment. **d**, Representative western blot from three independent experiments of PC3 cells after 48 h of *4EBP1*/*4EBP2* knockdown followed by 24-h INK128 treatment (see quantification of independent experiments in Supplementary Fig. 23a). **e**, Representative western blot from three independent experiments of wild type (WT) and *4EBP1*/*4EBP2* double knockout (DKO) MEFs treated with INK128 for 24 h. **f**, Representative western blot from two independent experiments of wild-type and *mSin1*$^{-/-}$ (also called *Mapkap1*^{tm1Bisu}) MEFs after 24-h INK128 treatment. **g**, Matrigel invasion assay upon 48-h doxycycline induction of 4EBP1^{M}, or treatment with DG-2 compared to control ($n = 6$ per condition, *t*-test). All data represent mean ± s.e.m.

prostate epithelial cell line, increased the invasive capacity of these cells in an additive manner (Fig. 2e). Notably, the effects of YB1 and MTA1 on cell invasion are independent from any effect on cell proliferation in both knockdown or overexpression studies (Supplementary Fig. 21b, c). Therefore, translational control of pro-invasion mRNAs by oncogenic mTOR signalling alters the ability of epithelial cells to migrate and invade, a key feature of cancer metastasis.

Dissecting mTOR translational effectors

We sought to determine the molecular mechanism by which pro-invasion genes are regulated at the translational level and why these mRNAs are sensitive to INK128 but not rapamycin. To this end, we investigated whether the translational regulators downstream mTORC1, 4EBP1 and/or p70S6K1/2, control the expression of these mTOR-sensitive targets. We generated a human prostate cancer cell line that stably expresses a doxycycline-inducible dominant-negative mutant of 4EBP1 ($4EBP1^{M}$) (Fig. 3a)[13]. This mutant binds to eIF4E, decreasing its hyperactivation without inhibiting general mTORC1 function (Supplementary Fig. 22a). Notably, expression of $4EBP1^{M}$ does not alter global protein synthesis (Supplementary Fig. 22b), probably because endogenous 4EBP1 and 4EBP2 proteins retain their ability to bind to eIF4E (Supplementary Fig. 22c)[13]. Upon induction of $4EBP1^{M}$, YB1, vimentin, CD44 and MTA1 decrease at the protein but not mRNA level, whereas pharmacological inhibition of p70S6K1/2 with DG-2 (ref. 23) had no effect (Fig. 3b, c and Supplementary Fig. 22d). Next, we tested whether INK128 decreases expression of the four invasion genes through the 4EBP–eIF4E axis. Notably, knockdown of *4EBP1* and *4EBP2* in PC3 cells or using *4EBP1* and *4EBP2* double knockout mouse embryonic fibroblasts (MEFs)[24] reduced the ability of INK128 to decrease expression of these pro-invasion mRNAs (Fig. 3d, e and Supplementary Fig. 23). Furthermore, ablation of mTORC2 activity[25] had no effect on the expression of these mRNAs or responsiveness to INK128 (Fig. 3f and Supplementary Fig. 24a–c). Next, we determined the effect of $4EBP1^{M}$ on human prostate cancer cell invasion. The expression of $4EBP1^{M}$ resulted in a significant decrease in prostate cancer cell invasion without affecting the cell cycle, whereas DG-2 had no effect (Fig. 3g and Supplementary Fig. 24d). These findings demonstrate that eIF4E hyperactivation downstream of oncogenic mTOR regulates translational control of the pro-invasion mRNAs and provides an explanation for the selective targeting of this gene signature by mTOR ATP site inhibitors.

Examining cell invasion networks *in vivo*

Both $CK5^{+}$ and $CK8^{+}$ prostate epithelial cells have been implicated in the initiation of prostate cancer upon loss of PTEN[26,27]. *Pten*$^{loxp/loxp}$;*Pb-cre* ($Pten^{L/L}$) mice are an ideal model of prostate cancer because they display distinct stages of cancer development (prostatic intraepithelial neoplasia, invasive adenocarcinoma, and metastasis)[28]. However, the expression patterns of YB1, vimentin, CD44 and MTA1 in prostate basal ($CK5^{+}$) and luminal ($CK8^{+}$) epithelial cells have not been characterized. We therefore analysed their expression patterns in the $Pten^{L/L}$ prostate cancer mouse model, where mTOR is constitutively hyperactivated[9,28]. We found that YB1 localizes to the cytoplasm and nucleus of $CK5^{+}$ and $CK8^{+}$ prostate epithelial cells, consistent with its ability to shuttle between the two cellular compartments (Fig. 4a, b and Supplementary Fig. 25a, b)[18,29]. MTA1 expression is exclusively nuclear in both cell types (Fig. 4c, d). Of note, CD44, together with other cell-surface markers, has been used to isolate a rare prostate stem-cell population[30]. We observed expression of CD44 within a subset of $CK5^{+}$ and $CK8^{+}$ epithelial cells (Fig. 4e, f). In contrast, vimentin is not detected in either cell type (Fig. 4g). We next determined the impact of mTOR hyperactivation on the expression pattern of the pro-invasion gene signature. YB1, MTA1 and CD44 protein, but not transcript, levels were significantly increased in both $Pten^{L/L}$ luminal and basal epithelial cells compared to wild type (Fig. 4h and Supplementary Fig. 25c–e). Interestingly, a subset of $Pten^{L/L}$ luminal epithelial cells ectopically expresses vimentin at aberrantly high levels, with a perinuclear distribution (Fig. 4g and Supplementary Fig. 25f, g) suggesting that these cells may have acquired some mesenchymal-like features. Consistent with these findings, perinuclear vimentin localization is associated with invasive features of human prostate cancer cells[31] and changes

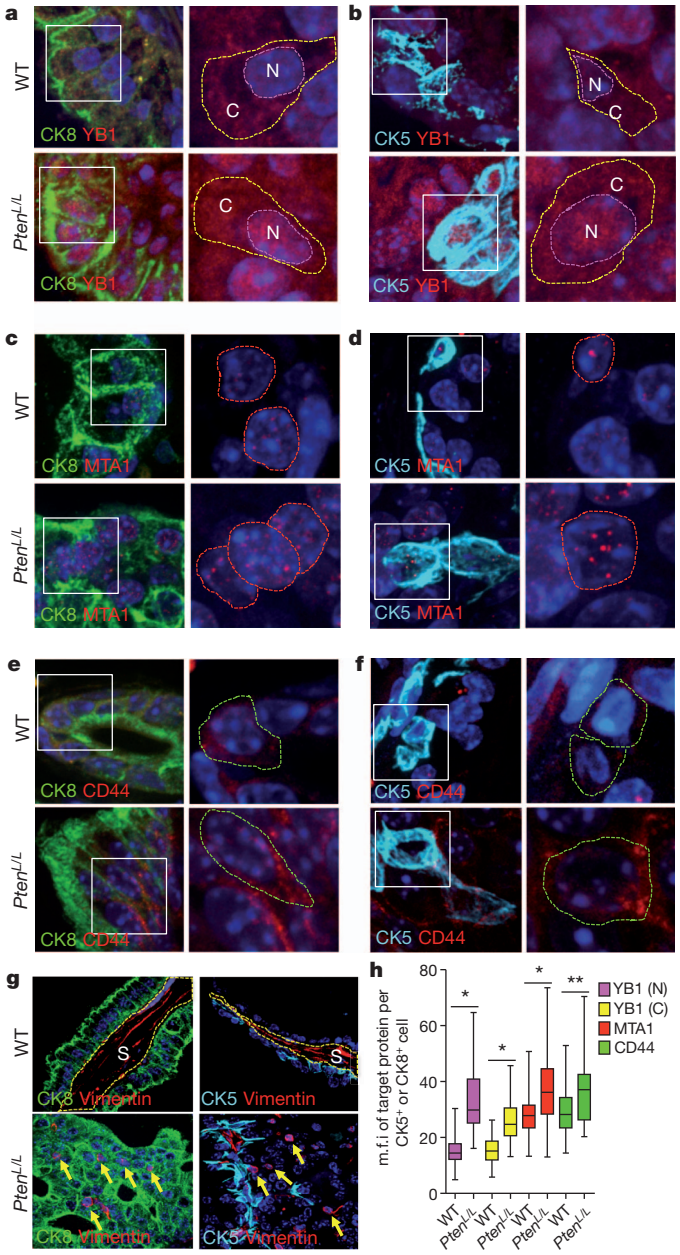

Figure 4 | mTOR hyperactivation augments translation of *YB1*, *MTA1*, *CD44* and vimentin mRNAs in a subset of pre-invasive prostate cancer cells *in vivo*. Left: immunofluorescent images of CK8/DAPI or CK5/DAPI with YB1 (**a**, **b**), MTA1 (**c**, **d**), or CD44 (**e**, **f**) co-staining in 14-month-old wild-type and $Pten^{L/L}$ mouse prostate epithelial cells. White boxes outline the area magnified in the right panel. Right: magnified immunofluorescent images of YB1 (**a**, **b**), MTA1 (**c**, **d**) and CD44 (**e**, **f**) co-stained with DAPI in wild-type and $Pten^{L/L}$ mouse prostate epithelial cells. Dotted lines encircle the cytoplasm (C) and/or the nucleus (N). **g**, Representative immunofluorescent images of CK5 or CK8 co-staining with vimentin in 14-month-old wild-type and $Pten^{L/L}$ mouse prostate epithelial cells. S, stroma; yellow arrows indicate perinuclear vimentin. **h**, Box plot of YB1 (N = nuclear, C = cytoplasmic), MTA1 and CD44 mean fluorescence intensity (m.f.i.) per $CK5^{+}$ or $CK8^{+}$ prostate epithelial cell in wild-type and $Pten^{L/L}$ mice (three mice per arm, $n = 43$–303 cells quantified per target gene, error bars indicate range (see Supplementary Fig. 25b); $^{*}P < 0.0001$, $^{**}P = 0.0004$, *t*-test).

in cell polarity in actively moving fibroblasts[32]. These studies reveal a unique, translationally controlled signature of gene expression downstream of mTOR hyperactivation in a cancer-initiating subset of prostate epithelial cells.

Targeting prostate cancer metastasis

The most significant pre-clinical extension of this work would be to determine the therapeutic benefit of INK128 in reprogramming expression of the mTOR-dependent pro-invasion gene signature and prostate cancer metastasis directly *in vivo*. This is underscored by the clinical inefficacy of allosteric mTOR inhibition towards the lethal form of metastatic human prostate cancer[33,34]. Importantly, in our preclinical trial of RAD001 (rapalog) versus INK128 in $Pten^{L/L}$ mice, 4EBP1 and p70S6K1/2 phosphorylation was completely restored to wild-type levels after treatment with INK128, whereas RAD001 only decreased p70S6K1/2 phosphorylation levels (Supplementary Fig. 26a, b). We next determined the cellular consequences of complete versus partial mTOR inhibition during distinct stages of prostate cancer. INK128 treatment resulted in a 50% decrease in prostatic intraepithelial neoplasia (PIN) lesions in $Pten^{L/L}$ mice that was associated with decreased proliferation and a tenfold increase in apoptosis (Supplementary Fig. 26d–f). Notably,

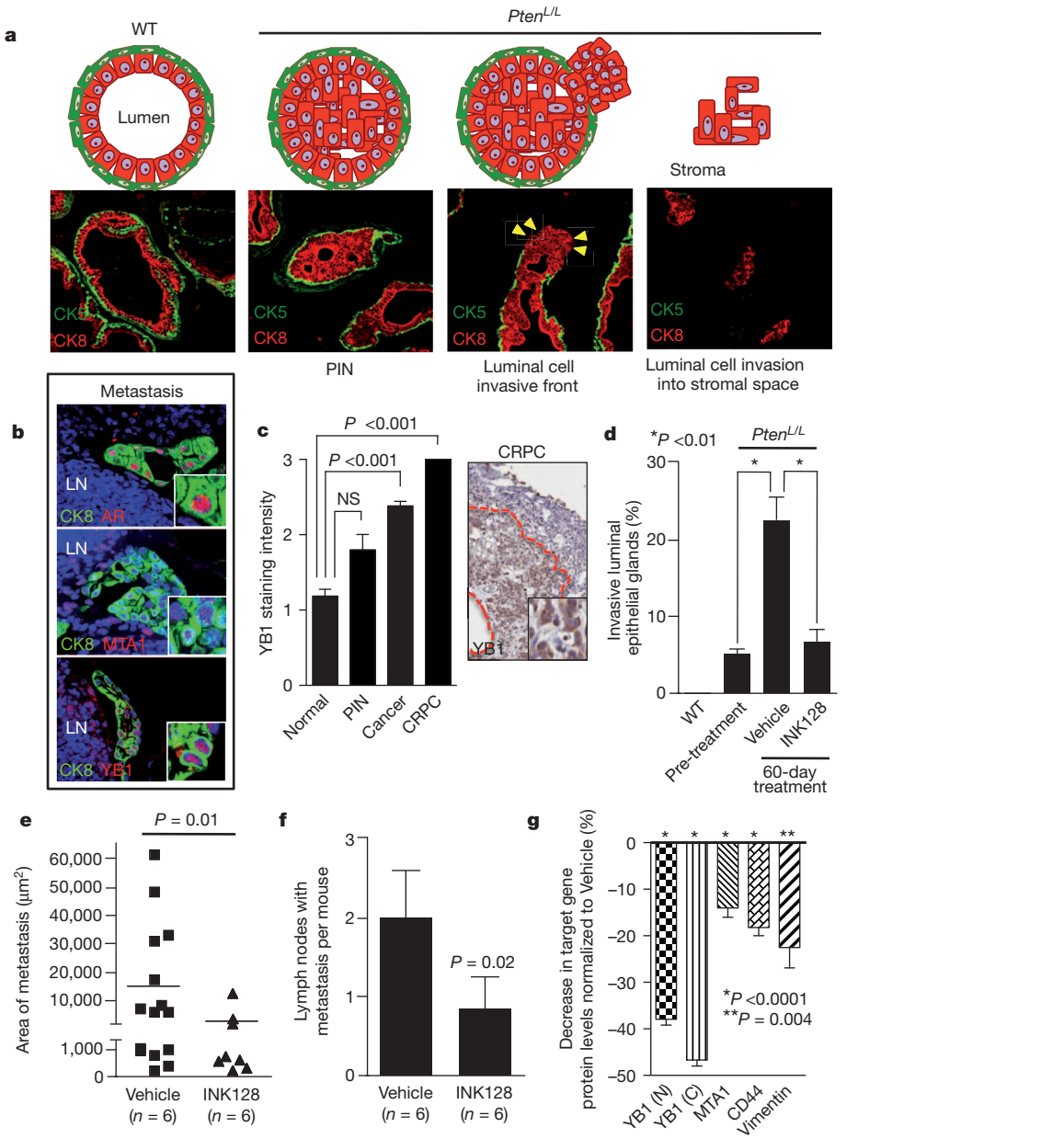

Figure 5 | Complete mTOR inhibition by INK128 treatment prevents prostate cancer invasion and metastasis *in vivo*. **a**, Diagram and images of normal prostate gland, pre-invasive PIN and invasive prostate cancer. CK8/CK5, luminal/basal epithelial cells, respectively. Yellow arrowheads indicate invasive front. **b**, Immunofluorescent images of 14-month-old $Pten^{L/L}$ lymph node (LN) metastasis co-stained with CK8/androgen receptor (AR), CK8/YB1 and CK8/MTA1. **c**, Left: human tissue microarray of YB1 protein levels in normal ($n = 59$), PIN ($n = 5$), cancer ($n = 99$) and CRPC ($n = 3$) (ANOVA). Right: immunohistochemistry of YB1 in human CRPC demarcated by the red line (inset shows nuclear and cytoplasmic YB1). **d**, Quantification of invasive prostate glands in wild-type and $Pten^{L/L}$ mice before (12-months old) and after (14-months old) 60 days of INK128 treatment ($n = 6$ mice per arm, ANOVA). **e**, **f**, Area and number of CK8/AR$^+$ metastases in draining lymph nodes in 14-month-old $Pten^{L/L}$ mice after 60 days of INK128 treatment ($n = 6$ mice per arm, *t*-test). **g**, Percentage decrease of YB1 (N = nuclear, C = cytoplasmic), MTA1, CD44, or vimentin protein levels (determined by quantitative immunofluorescence, Supplementary Fig. 25b) in CK8$^+$ or CK5$^+$ prostate cells (CK8$^+$ only for vimentin) in INK128-treated 14-month-old $Pten^{L/L}$ mice normalized to vehicle-treated mice ($n = 3$ mice per arm, *t*-test). All data represent mean ± s.e.m.

the unique cytotoxic properties of INK128 treatment in $Pten^{L/L}$ mice were evidenced by a marked reduction in prostate cancer volume. In addition, and consistent with these findings, INK128 induced programmed cell death in multiple cancer cell lines (Supplementary Fig. 27a, b). In contrast, RAD001 treatment mainly had cytostatic effects leading to only partial regression of PIN lesions associated with a limited decrease in cell proliferation and no significant effect on apoptosis (Supplementary Fig. 26c–f).

We extended the preclinical trial by examining the effects of INK128 treatment on the pro-invasion gene signature and prostate cancer metastasis, which is incurable and the primary cause of patient mortality. Cell invasion is the critical first step in metastasis, required for systemic dissemination. In $Pten^{L/L}$ mice after the onset of PIN, a subset of prostate glands show characteristics of luminal epithelial cell invasion by 12 months (Fig. 5a and Supplementary Fig. 27c)[28]. After 12 months of age, $Pten^{L/L}$ mice develop lymph-node metastases and these cells maintain strong YB1 and MTA1 expression (Fig. 5b). We further extended these findings directly to human prostate cancer patient specimens, observing that YB1 expression levels increase in a stepwise fashion from normal prostate to castration-resistant prostate cancer (CRPC), an advanced form of the disease associated with increased metastatic potential (Fig. 5c). MTA1 levels exhibit similar increases[20]. In human prostate cancer, high-grade primary tumours that display invasive features are more likely to develop systemic metastasis than low-grade non-invasive tumours[35,36]. Remarkably, treatment with INK128 completely blocked the progression of invasive prostate cancer locally in the prostate gland, and profoundly inhibited the total number and size of distant metastases (Fig. 5d–f). This was associated with a marked decrease in the expression of YB1, vimentin, CD44 and MTA1 at the protein, but not transcript, level in specific epithelial cell types within pre-invasive PIN lesions in $Pten^{L/L}$ mice (Fig. 5g and Supplementary Fig. 25c). Together, these findings reveal an unexpected role for oncogenic mTOR signalling in control of a pro-invasion translational program that, along with the lethal metastatic form of prostate cancer, can be efficiently targeted with clinically relevant mTOR ATP site inhibitors.

Discussion

Here we used ribosome profiling to generate a comprehensive map of translationally controlled mTOR targets in cancer that surprisingly stratify into specific cellular processes including proliferation, metabolism, protein synthesis and invasion (Fig. 1e). The effects of this translational control program are probably broad, converging on many subclasses of mRNAs that may cooperate towards distinct steps in cancer development and therapeutic response. This is supported by our *in vivo* findings where we developed a novel clinically relevant mTOR inhibitor, INK128, that significantly abrogates multiple aspects of prostate cancer development by inducing apoptosis as well as inhibiting cell proliferation, invasion and metastasis (Fig. 5d–g and Supplementary Fig. 26c–f). The superiority of INK128 as an mTOR inhibitor is also evident in its ability to reprogram the mTOR oncogenic translational program in prostate cancer, which is not achieved by rapalog treatment. Of note, however, the sensitivity of cells from distinct histological origins to ATP site versus allosteric inhibitors of mTOR may differ. For example, the Jurkat lymphoid cell line is particularly sensitive to rapamycin treatment[37].

One of the most novel nodes of mTOR translationally controlled genes are those that cooperatively control, at least in part, the cellular invasive features of human prostate cancer cells (Figs 1g, 2 and 3b, g). Translational control of these mRNAs relies on the 4EBP1–eIF4E axis and is thereby specifically druggable with potent mTOR ATP site inhibitors, which, unlike rapamycin, target mTOR-dependent 4EBP1 phosphorylation (Figs 1g, 3d, e and 5g, and Supplementary Figs 1b, 23 and 26b). This has significant therapeutic implications not only for advanced prostate cancer but also for multiple metastatic cancers where we show that translational control of pro-invasion mRNAs is sensitive to ATP site inhibitors of mTOR (Supplementary Fig. 16). Thereby, these studies link translational regulation to the poorly understood mechanisms underlying cancer metastasis. Intriguingly, various components of the translation machinery, including oncogenic eIF4E[38], localize to the leading edge of migrating fibroblasts[39]. This may allow spatially controlled translation of mRNAs important for cell migration, providing a rapid and specific response in transducing a migration program that could be co-opted at the invasive edge of metastatic cancer cells. Together, these studies reveal that the ability of mTOR to phosphorylate general translation factors results in exquisite transcript-specific translational control of key mRNAs that may cooperate in distinct steps of cancer initiation and progression, with significant implications for therapeutic intervention.

METHODS SUMMARY

Mice. $Pten^{loxp/loxp}$ and *Pb-cre* mice were obtained from Jackson Laboratories and Mouse Models of Human Cancers Consortium (MMHCC) and maintained in the C57BL/6 background.

Ribosome profiling. PC3 lysates were subjected to ribosome footprinting by nuclease treatment. Ribosome-protected and alkaline digested poly(A) mRNA fragments were purified and deep sequencing libraries were generated. Ribosome footprint and RNA-seq sequencing reads were aligned against a library of transcripts from the UCSC Known Genes database GRCh37/hg19. Read density profiles were constructed for the canonical transcript of each gene. The average read density per codon was computed for the coding sequence of each transcript. Average read density was used to determine mRNA abundance (RNA-seq reads), ribosome occupancy of mRNAs (foot print reads), and translational efficiency (foot print reads/RNA-seq reads).

Immunofluorescence. Paraffin-embedded mouse prostates and lymph nodes were deparaffinized and rehydrated using CitriSolv (Fisher) and serial ethanol washes. Antigen unmasking was performed using Citrate pH 6 (Vector Labs). Sections were blocked in 5% goat serum, 1% BSA in TBS. Various primary antibodies were used at dilutions between 1:50 and 1:500 (see Methods), followed by incubation with appropriate conjugated secondary antibodies. Samples were mounted with DAPI Hardset Mounting Medium (Vector Lab). A Zeiss Spinning Disc confocal (Zeiss, CSU-X1) was used to image the tissues. Individual cells were quantified for mean fluorescence intensity using the Axiovision (Zeiss, Release 4.8) densitometric tool.

Full Methods and any associated references are available in the online version of the paper at www.nature.com/nature.

Received 14 July 2011; accepted 3 February 2012.
Published online 22 February 2012.

1. Brown, E. J. *et al.* Control of p70 s6 kinase by kinase activity of FRAP *in vivo*. *Nature* **377,** 441–446 (1995).
2. Gingras, A. C., Kennedy, S. G., O'Leary, M. A., Sonenberg, N. & Hay, N. 4E–BP1, a repressor of mRNA translation, is phosphorylated and inactivated by the Akt(PKB) signaling pathway. *Genes Dev.* **12,** 502–513 (1998).
3. Kim, D. H. *et al.* mTOR interacts with raptor to form a nutrient-sensitive complex that signals to the cell growth machinery. *Cell* **110,** 163–175 (2002).
4. Sarbassov, D. D. *et al.* Rictor, a novel binding partner of mTOR, defines a rapamycin-insensitive and raptor-independent pathway that regulates the cytoskeleton. *Curr. Biol.* **14,** 1296–1302 (2004).
5. Gingras, A. C., Raught, B. & Sonenberg, N. Regulation of translation initiation by FRAP/mTOR. *Genes Dev.* **15,** 807–826 (2001).
6. Ruvinsky, I. & Meyuhas, O. Ribosomal protein S6 phosphorylation: from protein synthesis to cell size. *Trends Biochem. Sci.* **31,** 342–348 (2006).
7. Ingolia, N. T., Ghaemmaghami, S., Newman, J. R. & Weissman, J. S. Genome-wide analysis *in vivo* of translation with nucleotide resolution using ribosome profiling. *Science* **324,** 218–223 (2009).
8. Taylor, B. S. *et al.* Integrative genomic profiling of human prostate cancer. *Cancer Cell* **18,** 11–22 (2010).
9. Nardella, C. *et al.* Differential requirement of mTOR in postmitotic tissues and tumorigenesis. *Sci. Signal.* **2,** ra2 (2009).
10. Guertin, D. A. *et al.* mTOR complex 2 is required for the development of prostate cancer induced by Pten loss in mice. *Cancer Cell* **15,** 148–159 (2009).
11. Furic, L. *et al.* eIF4E phosphorylation promotes tumorigenesis and is associated with prostate cancer progression. *Proc. Natl Acad. Sci. USA* **107,** 14134–14139 (2010).
12. Feldman, M. E. *et al.* Active-site inhibitors of mTOR target rapamycin-resistant outputs of mTORC1 and mTORC2. *PLoS Biol.* **7,** e38 (2009).
13. Hsieh, A. C. *et al.* Genetic dissection of the oncogenic mTOR pathway reveals druggable addiction to translational control via 4EBP-eIF4E. *Cancer Cell* **17,** 249–261 (2010).

14. Tang, H. *et al.* Amino acid-induced translation of TOP mRNAs is fully dependent on phosphatidylinositol 3-kinase-mediated signaling, is partially inhibited by rapamycin, and is independent of S6K1 and rpS6 phosphorylation. *Mol. Cell. Biol.* **21,** 8671–8683 (2001).
15. Meyuhas, O. Synthesis of the translational apparatus is regulated at the translational level. *Eur. J. Biochem.* **267,** 6321–6330 (2000).
16. Crosio, C., Boyl, P. P., Loreni, F., Pierandrei-Amaldi, P. & Amaldi, F. La protein has a positive effect on the translation of TOP mRNAs *in vivo*. *Nucleic Acids Res.* **28,** 2927–2934 (2000).
17. Ørom, U. A., Nielsen, F. C. & Lund, A. H. MicroRNA-10a binds the 5′UTR of ribosomal protein mRNAs and enhances their translation. *Mol. Cell* **30,** 460–471 (2008).
18. Evdokimova, V. *et al.* Translational activation of snail1 and other developmentally regulated transcription factors by YB-1 promotes an epithelial-mesenchymal transition. *Cancer Cell* **15,** 402–415 (2009).
19. Lahat, G. *et al.* Vimentin is a novel anti-cancer therapeutic target; insights from *in vitro* and *in vivo* mice xenograft studies. *PLoS ONE* **5,** e10105 (2010).
20. Hofer, M. D. *et al.* The role of metastasis-associated protein 1 in prostate cancer progression. *Cancer Res.* **64,** 825–829 (2004).
21. Yoo, Y. G., Kong, G. & Lee, M. O. Metastasis-associated protein 1 enhances stability of hypoxia-inducible factor-1α protein by recruiting histone deacetylase 1. *EMBO J.* **25,** 1231–1241 (2006).
22. Liu, C. *et al.* The microRNA miR-34a inhibits prostate cancer stem cells and metastasis by directly repressing CD44. *Nature Med.* **17,** 211–215 (2011).
23. Okuzumi, T. *et al.* Inhibitor hijacking of Akt activation. *Nature Chem. Biol.* **5,** 484–493 (2009).
24. Dowling, R. J. *et al.* mTORC1-mediated cell proliferation, but not cell growth, controlled by the 4E-BPs. *Science* **328,** 1172–1176 (2010).
25. Jacinto, E. *et al.* SIN1/MIP1 maintains rictor-mTOR complex integrity and regulates Akt phosphorylation and substrate specificity. *Cell* **127,** 125–137 (2006).
26. Wang, X. *et al.* A luminal epithelial stem cell that is a cell of origin for prostate cancer. *Nature* **461,** 495–500 (2009).
27. Mulholland, D. J. *et al.* $Lin^{-}Sca\text{-}1^{+}CD49f^{high}$ stem/progenitors are tumor-initiating cells in the Pten-null prostate cancer model. *Cancer Res.* **69,** 8555–8562 (2009).
28. Wang, S. *et al.* Prostate-specific deletion of the murine Pten tumor suppressor gene leads to metastatic prostate cancer. *Cancer Cell* **4,** 209–221 (2003).
29. Sutherland, B. W. *et al.* Akt phosphorylates the Y-box binding protein 1 at Ser102 located in the cold shock domain and affects the anchorage-independent growth of breast cancer cells. *Oncogene* **24,** 4281–4292 (2005).
30. Leong, K. G., Wang, B. E., Johnson, L. & Gao, W. Q. Generation of a prostate from a single adult stem cell. *Nature* **456,** 804–818 (2008).
31. Lang, S. H. *et al.* Enhanced expression of vimentin in motile prostate cell lines and in poorly differentiated and metastatic prostate carcinoma. *Prostate* **52,** 253–263 (2002).
32. Helfand, B. T. *et al.* Vimentin organization modulates the formation of lamellipodia. *Mol. Biol. Cell* **22,** 1274–1289 (2011).
33. Amato, R. J., Jac, J., Mohammad, T. & Saxena, S. Pilot study of rapamycin in patients with hormone-refractory prostate cancer. *Clin. Genitourin. Cancer* **6,** 97–102 (2008).
34. George, D. J. *et al.* A phase II study of RAD001 in men with hormone refractory metastatic prostate cancer (HRPC). *Am. Soc. Clin. Oncol. Genitourin. Cancers Symp*. Abstract 181 (2008).
35. Pontes, J. E., Wajsman, Z., Huben, R. P., Wolf, R. M. & Englander, L. S. Prognostic factors in localized prostatic carcinoma. *J. Urol.* **134,** 1137–1139 (1985).
36. Zhou, P. *et al.* Predictors of prostate cancer-specific mortality after radical prostatectomy or radiation therapy. *J. Clin. Oncol.* **23,** 6992–6998 (2005).
37. Grolleau, A. *et al.* Global and specific translational control by rapamycin in T cells uncovered by microarrays and proteomics. *J. Biol. Chem.* **277,** 22175–22184 (2002).
38. Ruggero, D. R. *et al.* The translation factor eIF-4F promotes tumor formation and cooperates with c-Myc in lymphomagenesis. *Nature Med.* **10,** 484–486 (2004).
39. Willett, M., Brocard, M., Davide, A. & Morley, S. J. Translation initiation factors and active sites of protein synthesis co-localize at the leading edge of migrating fibroblasts. *Biochem. J.* **438,** 217–227 (2011).

Supplementary Information is linked to the online version of the paper at www.nature.com/nature.

Acknowledgements We thank M. Barna for critical discussion and reading of this manuscript; T. Wilson for support and advice; T. Sanders and E. Llagostera-Martin for technical support with confocal microscopy; L. Li, E. Ulm, L. Kessler, J. Kucharski and L. Darjania for technical support for the discovery and development of INK128. J. Kurhanewicz and R. Bok of the Surbeck Institute for Advanced Imaging for technical support and MRI images; N. Sonenberg for providing the 4EBP1/2 double knockout mouse embryonic fibroblasts; J. M. Shen for support; and K. Tong for editing the manuscript. A.C.H. is supported in part by the American Cancer Society (119084-PF-10-233-01-TBE), and is a Prostate Cancer Foundation Young Investigator, and a recipient of the DOD Prostate Cancer Training Award. This work is supported by NIH R01 CA154916 (D.R.), NIH R01 CA140456 (D.R.) and the Phi Beta Psi Sorority (D.R.). D.R. is a Leukemia & Lymphoma Society Scholar.

Author Contributions A.C.H. and D.R. conceived the experiments. A.C.H., M.P.E., M.R.J., A.S., E.Y.S., C.R.S., C.C. and S.W. performed the experiments, *Pten*$^{L/L}$ preclinical trials, and collected the data. N.T.I. and J.S.W. contributed to ribosomal profiling data analysis. M.J.B. provided pathology support. Y.L., P.R., M.M., S.W., K.J., M.E.F., K.M.S. and C.R. developed and/or supported development of INK128, conducted pharmacokinetic, pharmacodynamic and preclinical studies. A.C.H. and D.R. analysed the data and wrote the manuscript. All authors discussed results and edited the manuscript.

Author Information Small-RNA sequencing data were deposited in the Gene Expression Omnibus (http://www.ncbi.nlm.nih.gov/geo/) under accession number GSE35469. Reprints and permissions information is available at www.nature.com/reprints. The authors declare competing financial interests: details accompany the full-text HTML version of the paper at www.nature.com/nature. Readers are welcome to comment on the online version of this article at www.nature.com/nature. Correspondence and requests for materials should be addressed to D.R. (davide.ruggero@ucsf.edu) or C.R. (christian@intellikine.com).

METHODS

Mice. *Pten*$^{loxp/loxp}$ and *Pb-cre* mice where obtained from Jackson Laboratories and Mouse Models of Human Cancers Consortium (MMHCC), respectively, and maintained in the C57BL/6 background. Mice were maintained under specific pathogen-free conditions, and experiments were performed in compliance with institutional guidelines as approved by the Institutional Animal Care and Use Committee of UCSF.

Cell culture and reagents. Human cell lines were obtained from the ATCC and maintained in the appropriate medium with supplements as suggested by ATCC. Wild-type, *mSin1*$^{-/-}$ (provided by B. Su), and *4EBP1*/*4EBP2* double knockout MEFs (provided by N. Sonenberg) were cultured as previously described[24,25]. SMARTvector 2.0 (Thermo Scientific) lentiviral shRNA constructs were used to knock down PTEN (SH-003023-02-10). For generation of GFP-labelled PC3 cells, SMARTvector 2.0 lentiviral empty vector control particles that contain TurboGFP (S-004000-01) were used. Control (D-001810-01), *YB1* (L-010213), *MTA1* (L-004127), *CD44* (L-009999), vimentin (L-003551), rictor (LL-016984), *4EBP1* (L-003005) and *4EBP2* (L-018671) pooled siRNAs were purchased from Thermo Scientific. Intellikine provided INK128 and PP242, which were used at 200 nM and 2.5 μM in cell-based assays unless otherwise specified. RAD001 was obtained from LC Laboratories. DG-2 was provided by K. Shokat and used at 20 μM in cell-based assays. Rapamycin was purchased from Calbiochem and used at 50 nM in cell-based assays. Doxycyline (Sigma) was used at 1 μg ml^{-1} in 4EBP1^{M} induction assays. Lipofectamine 2000 (Invitrogen) was used to transfect cancer cell lines with siRNA. Amaxa Cell Line Nucleofector Kit R (Lonza) was used to electroporate BPH-1 cells with over expression vectors. The 4EBP1^{M} has been previously described[13].

Plasmids. pcDNA3-HA-YB1 was provided by V. Evdokimova. pCMV6-Myk-DDK-MTA1 was purchased from Origene. pGL3-Promoter was purchased from Promega. To clone the 5′ UTR of *YB1* into pGL3-Promoter, the entire 5′ UTR sequence of *YB1* was amplified from PC3 cDNA. PCR fragments were digested with HindIII and NcoI and ligated into the corresponding sites of pGL3-Promoter. The PRTE sequence at position +20–34 in the *YB1* 5′ UTR (UCSC kgID uc001chs.2) was mutated using the QuikChange Site-Directed Mutagenesis Kit following the manufacturer's protocol (Stratagene).

Ribosome profiling. PC3 cells were treated with rapamycin (50 nM; Calbiochem) or PP242 (2.5 μM; Intellikine) for 3 h. Cells were subsequently treated with cycloheximide (100 μg ml^{-1}; Sigma) and detergent lysis was performed in the dish. The lysate was treated with DNase and clarified, and a sample was taken for RNA-seq analysis. Lysates were subjected to ribosome foot printing by nuclease treatment. Ribosome-protected fragments were purified, and deep sequencing libraries were generated from these fragments, as well as from poly(A) mRNA purified from non-nuclease-treated lysates. These libraries were analysed by sequencing on an Illumina GAII.

Each sequencing run resulted in approximately 20–25 million raw reads per sample, of which 5–12 million unique reads were used for subsequent analysis. Ribosome footprint and RNA-seq sequencing reads were aligned against a library of transcripts from the UCSC Known Genes database GRCh37/hg19. The first 25 nucleotides of each read were aligned using Bowtie and this initial alignment was then extended to encompass the full fragment-derived portion of the sequencing read while excluding the linker sequence. Read density profiles were then constructed for the canonical transcript of each gene, using only reads with 0 or 1 total mismatches between the read sequence and the reference sequence, comprised of the transcript fragment followed by the linker sequence. Footprint reads were assigned to an A site nucleotide at position +15 to +17 of the alignment, based on the total fragment length; mRNA reads were assigned to the first nucleotide of the alignment. The average read density per codon was then computed for the coding sequence of each transcript, excluding the first 15 and last 5 codons, which can display atypical ribosome accumulation.

Average read density was used as a measure of mRNA abundance (RNA-seq reads) and of protein synthesis (ribosome profiling reads). For most analyses, genes were filtered to require at least 256 reads in the relevant RNA-seq samples. Translational efficiency was computed as the ratio of ribosome footprint read density to RNA-seq read density, scaled to normalize the translational efficiency of the median gene to 1.0 after excluding regulated genes ($\log_2$ fold-change ±1.5 after normalizing for the all-gene median). Changes in protein synthesis, mRNA abundance and translational efficiency were similarly computed as the ratio of read densities between different samples, normalized to give the median gene a ratio of 1.0. This normalization corrects for differences in the absolute number of sequencing reads obtained for different libraries. 3,977 (replicate 1), and 5,333 (replicate 2) unique mRNAs passed a preset read threshold of 256 reads for single-gene quantification for all treatment conditions.

Western blot analysis. Western blot analysis was performed as previously described[13] with antibodies specific to phospho-AKT^{S473} (Cell Signaling), AKT (Cell Signaling), phospho-p70S6K^{T389} (Cell Signaling), phospho-rpS6$^{S240/244}$ (Cell Signaling), rpS6 (Cell Signaling), phospho-4EBP1$^{T37/46}$ (Cell Signaling), 4EBP1 (Cell Signaling), 4EBP2 (Cell Signaling), YB1 (Cell Signaling), CD44 (Cell Signaling), LEF1 (Cell Signaling), PTEN (Cell Signaling), eEF2 (Cell Signaling), GAPDH (Cell Signaling), vimentin (BD Biosciences), eIF4E (BD Biosciences), Flag (Sigma), β-actin (Sigma), MTA1 (Santa Cruz Biotechnology), Twist (Santa Cruz Biotechnology), rpL28 (Santa Cruz Biotechnology), HA (Covance) and rictor (Bethyl Laboratory).

qPCR analysis. RNA was isolated using the manufacturer's protocol for RNA extraction with TRIzol Reagent (Invitrogen) using the Pure Link RNA mini kit (Invitrogen). RNA was Dnase-treated with Pure Link Dnase (Invitrogen). Dnase-treated RNA was transcribed to cDNA with SuperScript III First-Strand Synthesis System for RT–PCR (Invitrogen), and 1 μl of cDNA was used to run a SYBR green detection qPCR assay (SYBR Green Supermix and MyiQ2, Biorad). Primers were used at 200 nM.

5′ UTR analysis. 5′ UTRs of the 144 downregulated mTOR target genes were obtained using the known gene ID from the UCSC Genome Browser (GRCh37/hg19). Target versus non-target mRNAs were compared for 5′ UTR length, %G+C content and Gibbs free energy by the Wilcoxon two-sided test. Multiple E_m (expectation maximization) for Motif Elicitation (MEME) and Find Individual Motif Occurrences (FIMO) was used to derive the PRTE and determine its enrichment in the 144 mTOR-sensitive genes compared a background list of 3,000 genes. The Database of Transcriptional Start Sites (DBTSS Release 8.0) was used to identify putative 5′ TOP genes and putative transcription start sites in the 144 mTOR target genes.

Luciferase assay. PC3 4EBP1^{M} cells were treated with 1 μg ml^{-1} doxycycline (Sigma) for 24 h. Cells were transfected with various pGL3-Promoter constructs using lipofectamine 2000 (Invitrogen). After 24 h, cells were collected. 20% of the cells were aliquoted for RNA isolation. The remaining cells were used for the luciferase assay per the manufacturer's protocol (Promega). Samples were measured for luciferase activity on a Glomax 96-well plate luminometer (Promega). Firefly luciferase activity was normalized to luciferase mRNA expression levels.

Kinase assays. mTOR activity was assayed using LanthaScreen Kinase kit reagents (Invitrogen) according to the manufacturer's protocol. PI(3)K α, β, γ and δ activity were assayed using the PI(3)K HTRF assay kit (Millipore) according to the manufacturer's protocol. The concentration of INK128 necessary to achieve inhibition of enzyme activity by 50% (IC_{50}) was calculated using concentrations ranging from 20 μM to 0.1 nM (12-point curve). IC_{50} values were determined using a nonlinear regression model (GraphPad Prism 5).

Cell proliferation assay. PC3 cells were treated with the appropriate drug for 48 h, and proliferation was measured using CellTiter-Glo Luminescent reagent (Promega) per the manufacturer's protocol. The concentration of INK128 necessary to achieve inhibition of cell growth by 50% (IC_{50}) was calculated using concentrations ranging from 20.0 μM to 0.1 nM (12-point curve).

Mouse xenograft study. Nude mice were inoculated subcutaneously in the right subscapular region with 5×10^6 MDA-MB-361 cells. After tumours reached a size of 150–200 mm^3, mice were randomly assigned into vehicle control or treatment groups. INK128 was formulated in 5% polyvinylpropyline, 15% NMP, 80% water and administered by oral gavage at 0.3 mg kg^{-1} and 1 mg kg^{-1} daily.

Pharmacokinetic analysis. The area under the plasma drug concentration versus time curves, $AUC_{(0-t_{last})}$ and $AUC_{(0-inf)}$, were calculated from concentration data using the linear trapezoidal rule. The terminal $t_{1/2}$ in plasma was calculated from the elimination rate constant (lz), estimated as the slope of the log-linear terminal portion of the plasma concentration versus time curve, by linear regression analysis. The bioavailability (F) was calculated using $F = (AUC_{(0-last),po} D_{i.v.})/(AUC_{(0-last),iv} D_{p.o.}) \times 100\%$, where $D_{i.v.}$ and $D_{p.o.}$ are intravenous and oral doses, respectively. C_{max} was a highest drug concentration in plasma after oral administration. T_{max} was the time at which C_{max} is observed after extravascular administration of drug. T_{last} was the last time point a quantifiable drug concentration can be measured.

Metabolic stability assay. *In vitro* metabolic stability of INK128 was evaluated after incubation with liver microsomes or liver S9 fractions from various species in the presence of NADPH. The half-life of INK128 was estimated by log linear regression analysis.

CYP assay. INK128 inhibition of CYP450 isoforms in human liver microsomes was determined with isoform-specific substrates at concentrations approximately equal to the concentration at which the rate of the reaction is half-maximal (K_m) for the individual isoforms: CYP1A2, CYP2C8, CYP2C9, CYP2C19, CYP2D6 and CYP3A4.

Pharmaceutical property assays. The percentage of protein binding of INK128 was determined in mouse, rat, dog, monkey and human plasma at CEREP. The IC_{50} for the inhibitory effect of INK128 on hERG potassium channel was determined at

CEREP. A Bacterial Reverse Mutation Assay (Ames test) was conducted at BioReliance.

Polysome analysis. PC3 cells were treated for 3 h with either DMSO or INK128 (100 nM). Cells were re-suspended in PBS containing 100 μg ml^{-1} cycloheximide (Sigma) and incubated on ice for 10 min. Cells were centrifuged at 300*g* for 5 min at 4 °C and lysed in 10 mM Tris-HCl pH 8, 140 mM NaCl, 5 mM $MgCl_2$, 640 U ml^{-1} Rnasin, 0.05% NP-40, 250 μg ml^{-1} cycloheximide, 20 mM DTT and protease inhibitors. Samples were incubated for 20 min on ice then centrifuged once for 5 min at 3,300*g* and once for 5 min at 9,300*g*, isolating the supernatant after each centrifugation. Lysates were loaded onto 10–50% sucrose gradients containing 0.1 mg ml^{-1} heparin and 2 mM DTT and centrifuged at 37,000 r.p.m. for 2.5 h at 4 °C. The sample was subsequently fractionated on a gradient fractionation system (ISCO). RNA was extracted from all fractions and run on a TBE-agarose gel to visualize 18S and 28S rRNA. Fractions 7–13 were found to correspond to the polysome fractions and were used for further qPCR analysis.

[^{35}S] metabolic labelling. PC3 or PC3 4EBP1^{M} cells with or without indicated treatment were incubated with 30 μCi of [^{35}S]-methionine for 1 h after pre-incubation in methionine-free DMEM (Invitrogen). Cells were prepared using a standard protein lysate protocol, resolved on a 10% SDS polyacrylamide gel and transferred onto a PVDF membrane (Biorad). The membrane was exposed to autoradiography film (Denville) for 24 h and developed.

Cell cycle analysis. Appropriately treated PC3, BPH-1, or PC3-4EBP1^{M} cells were fixed in 70% ethanol overnight at −20 °C. Cells were subsequently washed with PBS and treated with RNase (Roche) for 30 min. After this incubation, the cells were permeabilized and treated with 50 μg ml^{-1} propidium iodide (Sigma) in a solution of 0.1% Tween, 0.1% sodium citrate. Cell cycle data was acquired using a BD FACS Caliber (BD Biosciences) and analysed with FlowJo (v.9.1).

Apoptosis analysis. Appropriately treated LNCaP and A498 cells were labelled with Annexin V-FITC (BD Biosciences) and propidium iodide (Sigma) following the manufacturer's instructions. PI/Annexin data was acquired using a BD FACS Caliber (BD Biosciences) and analysed with FlowJo (v.9.1).

Matrigel invasion assay. BioCoat Matrigel Invasion Chambers (modified Boyden Chamber Assay; BD Biosciences) were used according to the manufacturer's instructions.

Real-time imaging of cell migration. Real-time imaging of GFP-labelled PC3 cells was performed in poly-D-lysine-coated chamber cover glass slides (Lab-Tek). PC3 GFP cells were plated and allowed to adhere for 24 h. Wells were wounded with a P200 pipette tip. The chamber slides were imaged with an IX81 Olympus wide-field fluorescence microscope equipped with a CO_2 and temperature controlled chamber and time-lapse tracking system. Images from DIC and GFP channels were taken every 2 min and processed using ImageJ (http://rsb.info.nih.gov/ij/) and analysed for cell migration with Manual Tracking (http://rsbweb.nih.gov/ij/plugins/track/track.html), using local maximum centring correction to maintain a centroid *xy* coordinate for each cell per frame over time. Tracking data was subsequently processed with the Chemotaxis and Migration tool from ibidi (http://www.ibidi.de/applications/ap_chemo.html) to create *xy* coordinate plots, velocity and distance measurements.

Snail1 immunocytochemistry. Appropriately transfected or treated PC3 cells were plated on a poly-L-lysine-coated chamber slide (Lab-Tek) and cultured for 48 h. Cells were fixed with 4% paraformaldehye (EMS), rinsed with PBS and permeabilized with 0.1% Triton X-100. The samples were blocked in 5% goat serum and then incubated with anti-Snail1 antibody (Cell Signaling) in 5% goat serum for 2 h at room temperature. Cells were washed with PBS and incubated with Alexa 594 anti-mouse antibody (Invitrogen) and DAPI (Invitrogen) for 2 h at room temperature. Specimens were again washed with PBS and subsequently mounted with Aqua Poly/Mount (Polysciences). Image capture and quantification were completed as described below (see Immunofluorescence).

Cap-binding assay. PC3 4EBP1^{M} cells were induced with doxycycline (1 μg ml^{-1}, Sigma) for 48 h, then collected and lysed in buffer A (10 mM Tris-HCl pH 7.6, 150 mM KCl, 4 mM $MgCl_2$, 1 mM DTT, 1 mM EDTA, and protease inhibitors, supplemented with 1% NP-40). Cell lysates were incubated overnight at 4 °C with 50 μl of the mRNA cap analogue m^{7}GTP-sepharose (GE Healthcare) in buffer A. The beads were washed with buffer A supplemented with 0.5% NP-40. Protein complexes were dissociated using 1× sample buffer, and resolved by SDS–PAGE and western blotted with the appropriate antibodies.

Pharmacological treatment of *Pten*$^{L/L}$ mice and MRI imaging. Nine- and twelve-month-old *Pten*$^{L/L}$ mice were gavaged daily with either vehicle (see mouse xenograft study), RAD001 (10 mg kg^{-1}; LC Laboratories), or INK128 (1 mg kg^{-1}; Intellikine) for the indicated times. Weight measurements were taken every 3 days to monitor for toxicity. For the 28-day study, mice were imaged via MRI at day 0 and day 28 in a 14-T GE MR scanner (GE Healthcare).

Prostate tissue processing. Whole mouse prostates were removed from wild-type and *Pten*$^{L/L}$ mice, microdissected, and frozen in liquid nitrogen. Frozen tissues were subsequently manually disassociated using a biopulverizer (Biospec) and additionally processed for protein and mRNA analysis as described above.

Immunofluorescence. Prostates and lymph nodes were dissected from mice within 2 h of the indicated treatment and fixed in 10% formalin overnight at 4 °C. Tissues were subsequently dehydrated in ethanol (Sigma) at room temperature, mounted into paraffin blocks, and sectioned at 5 μm. Specimens were de-paraffinized and rehydrated using CitriSolv (Fisher) followed by serial ethanol washes. Antigen unmasking was performed on each section using Citrate pH 6 (Vector Labs) in a pressure cooker at 125 °C for 10–30 min. Sections were washed in distilled water followed by TBS washes. The sections were then incubated in 5% goat serum, 1% BSA in TBS for 1 h at room temperature. Various primary antibodies were used including those specific for keratin 5 (Covance), cytokeratin 8 (Abcam and Covance), YB1 (Abcam), vimentin (Abcam), MTA1 (Cell signaling), CD44 (BD Pharmingen) and the androgen receptor (Epitomics), which were diluted 1:50–1:500 in blocking solution and incubated on sections overnight at 4 °C. Specimens were then washed in TBS and incubated with the appropriate Alexa 488 and 594 labelled secondary (Invitrogen) at 1:500 for 2 h at room temperature with the exception of YB1 which was incubated with biotinylated anti-rabbit secondary (Vector) followed by incubation with Alexa 594 labelled Streptavidin (Invitrogen). A final set of washes in TBS was completed at room temperature followed by mounting with DAPI Hardset Mounting Medium (Vector Lab). A Zeiss Spinning Disc confocal (Zeiss, CSU-X1) was used to image the sections at 40×–100×. Individual prostate cells were quantified for mean fluorescence intensity (m.f.i.) using the Axiovision (Zeiss, Release 4.8) densitometric tool.

Lymph node metastasis measurements. Mouse lymph nodes were processed as described above and stained for CK8 and androgen receptor. Lymph nodes were imaged using a Zeiss AX10 microscope. Metastases were identified and areas were measured using the Axiovision (Zeiss, Release 4.8) measurement tool.

Semi-quantitative RT–PCR. Whole prostates were removed from wild-type and *Pten*$^{L/L}$ mice, microdissected, dissociated into single-cell suspension, and stained for epithelial cell markers as previously described[40] using fluorescence-conjugated antibodies for CD49f, Sca-1, CD31, CD45 and Ter119 (BD Biosciences). Luminal epithelial cells were sorted as previously described[41] using a FACS Aria (BD Biosciences). Cell pellets were re-suspended in 500 μl TRIzol Reagent and RNA was isolated and transcribed into cDNA as described above. Semi-quantitative PCR analysis was performed using oligonucleotides for vimentin and β-actin at 200 nM in a 25 μl reaction with 12.5 μl GoTaq (Promega) for 32 and 33 cycles respectively, which were within the linear range (Supplementary Fig. 25f).

Immunohistochemistry. Immunohistochemistry was performed as described above (see immunofluorescence section) with the exception that immediately after antigen presentation and TBS washes, specimens were incubated in 3% hydrogen peroxide in TBS followed by TBS washes. The following primary antibodies were used: phospho-AKT^{S473} (Cell Signaling), phospho-rpS6$^{S240/244}$ (Cell Signaling), phospho-4EBP1$^{T37/46}$ (Cell Signaling), phospho-histone H3 (Upstate), and cleaved caspase 3 (Cell Signaling). This was followed by TBS washes and incubation with the appropriate biotinylated secondary antibody (Vector Lab) for 30 min at room temperature. An ABC-HRP Kit (Vector Lab) was used to amplify the signal, followed by a brief incubation in hydrogen peroxide. The protein of interest was detected using DAB (Sigma). Specimens were counterstained with haematoxylin (Thermo Scientific), dehydrated with Citrisolv (Fisher), and mounted with Cytoseal XYL (Vector Lab).

Haematoxylin and eosin staining. Paraffin-embedded prostate specimens were deparaffinized and rehydrated as described above (see immunofluorescence section), stained with haematoxylin (Thermo Scientific), and washed with water. This was followed by a brief incubation in differentiation RTU (VWR) and two washes with water followed by two 70% ethanol washes. The samples were then stained with eosin (Thermo Scientific) and dehydrated with ethanol followed by CitriSolv (Fisher). Slides were mounted with Cytoseal XYL (Richard Allan Scientific).

Oligonucleotides. *YB1* 5′ UTR cloning and site-directed mutagenesis oligonucleotides are as follows. *YB1* 5′ UTR cloning: forward 5′-GCTACAAGCTTGGGCTTATCCCGCCT-3′, reverse 5′-TCGATCCATGGGGTTGCGGTGATGGT-3′; deletion (20–34): forward 5′-TGGGCTTATCCCGCCTGTCCTTCGATCGGTAGCGGGAGCG-3′, reverse 5′-CGCTCCCGCTACCGATCGAAGGACAGGCGGGATAAGCCCA-3′; transversion (20–34): forward 5′-TGGGCTTATCCCGCCTGTCCGCGGTAAGAGCGATCTTCGATCGGTAGCGGGAGCG-3′, reverse 5′-CGCTCCCGCTACCGATCGAAGATCGCTCTTACCGCGGACAGGCGGGATAAGCCCA-3′.

Human qPCR oligonucleotides are as follows. β-actin forward 5′-GCAAAGACCTGTACGCCAAC-3′, reverse 5′-AGTACTTGCGCTCAGGAGGA-3′; *CD44* forward 5′-CAACAACACAAATGGCTGGT-3′, reverse 5′-CTGAGGTGTCTGTCTCTTTCATCT-3′; vimentin forward 5′-GGCCCAGCTGTAAGTTGGTA-3′, reverse 5′-GGAGCGAGAGTGGCAGAG-3′; *Snail1* forward

5′-CACTATGCCGCGCTCTTTC-3′, reverse 5′-GCTGGAAGGTAAACTCTG GATTAGA-3′; *YB1* forward 5′-TCGCCAAAGACAGCCTAGAGA-3′, reverse 5′-TCTGCGTCGGTAATTGAAGTTG-3′; *MTA1* forward 5′-CAAAGTGGTG TGCTTCTACCG-3′, reverse 5′-CGGCCTTATAGCAGACTGACA-3′; *PLAU* forward 5′-TTGCTCACCACAACGACATT-3′, reverse 5′-GGCAGGCAGATG GTCTGTAT-3′; *FGFBP1* forward 5′-ACTGGATCCGTGTGCTCAG-3′, reverse 5′-GAGCAGGGTGAGGCTACAGA-3′; *ARID5B* forward 5′-TGGACTCAACT TCAAAGACGTTC-3′, reverse 5′-ACGTTCGTTTCTTCCTCGTC-3′; *CTGF* forward 5′-CTCCTGCAGGCTAGAGAAGC-3′, reverse 5′-GATGCACTTTT TGCCCTTCTT-3′; *RND3* forward 5′-AAAAACTGCGCTGCTCCAT-3′, reverse 5′-TCAAAACTGGCCGTGTAATTC-3′; *KLF6* forward 5′-AAAGCTC CCACTTGAAAGCA-3′, reverse 5′-CCTTCCCATGAGCATCTGTAA-3′; *BCL6* forward 5′-TTCCGCTACAAGGGCAAC-3′, reverse 5′-TGCAACGATA GGGTTTCTCA-3′; *FOXA1* forward 5′-AGGGCTGGATGGTTGTATTG-3′, reverse 5′-ACCGGGACGGAGGAGTAG-3′; *GDF15* forward 5′-CCGGATAC TCACGCCAGA-3′, reverse 5′-AGAGATACGCAGGTGCAGGT-3′; *HBP1* forward 5′-GCTGGTGGTGTTGTCGTG-3′, reverse 5′-CATGTTATGGTGCT CTGACTGC-3′; *Twist1* forward 5′-CATCCTCACACCTCTGCATT-3′, reverse 5′-TTCCTTTCAGTGGCTGATTG-3′; *LEF1* forward 5′-CCTTGGTGAACGA GTCTGAAATC-3′, reverse 5′-GAGGTTTGTGCTTGTCTGGC-3′; *rpS19* forward 5′-GCTGGCCAAACATAAAGAGC-3′, reverse 5′-CTGGGTCTGAC ACCGTTTCT-3′; 5S rRNA forward 5′-GCCCGATCTCGTCTGATCT-3′, reverse 5′-AGCCTACAGCACCCGGTATT-3′; firefly luciferase forward 5′-AATCAAAGAGGCGAACTGTG-3′, reverse 5′-TTCGTCTTCGTCCCAGT AAG-3′.

Mouse qPCR oligonucleotides are as follows. β-actin forward 5′-CTAAGG CCAACCGTGAAAAG-3′, reverse 5′-ACCAGAGGCATACAGGGACA-3′; *Yb1* forward 5′-GGGTTACAGACCACGATTCC-3′, reverse 5′-GGCGATACC GACGTTGAG-3′; vimentin forward 5′-TCCAGCAGCTTCCTGTAGGT-3′, reverse 5′-CCCTCACCTGTGAAGTGGAT-3′; *Cd44* forward 5′-ACAGTACCT TACCCACCATG-3′, reverse 5′-GGATGAATCCTCGGAATTAC-3′; *Mta1* forward 5′-AGTGCGCCTAATCCGTGGTG-3′, reverse 5′-CTGAGGATGAG AGCAGCTTTCG-3′.

siRNA/shRNA sequences are as follows. Control (D-001810-01) 5′-UGGU UUACAUGUCGACUAA-3′; vimentin (L-003551) 5′-UCACGAUGACCUUG AAUAA-3′, 5′-GGAAAUGGCUCGUCACCUU-3′, 5′-GAGGGAAACUAAU CUGGAU-3′, 5′-UUAAGACGGUUGAAACUAG-3′; *YB1* (L-010213) 5′-CUG AGUAAAUGCCGGCUUA-3′, 5′-CGACGCAGACGCCCAGAAA-3′, 5′-GUA AGGAACGGAUAUGGUU-3′, 5′-GCGGAGGCAGCAAAUGUUA-3′; *MTA1* (L-004127) 5′-UCACGGACAUUCAGCAAGA-3′, 5′-GGACCAAACCGCAG UAACA-3′, 5′-GCAUCUUGUUGGACAUAUU-3′, 5′-CCAGCAUCAUUGA GUACUA-3′; *CD44* (L-009999) 5′-GAAUAUAACCUGCCGCUUU-3′, 5′-CA AGUGGACUCAACGGAGA-3′, 5′-CGAAGAAGGUGUGGGCAGA-3′, 5′-GAUCAACAGUGGCAAUGGA-3′; *4EBP1* (L-003005) 5′-CUGAUGGAGU GUCGGAACU-3′, 5′-CAUCUAUGACCGGAAAUUC-3′, 5′-GCAAUAGCCC AGAAGAUAA-3′, 5′-GAGAUGGACAUUUAAAGCA-3′; *4EBP2* (L-018671) 5′-GCAGCUACCUCAUGACUAU-3′, 5′-GGAGGAACUCGAAUCAUUU-3′, 5′-GCAAUUCUCCCAUGGCUCA-3′, 5′-UUGAACAACUUGAACAA UC-3′; rictor (LL-016984) 5′-GACACAAGCACUUCGAUUA-3′, 5′-GAAGAU UUAUUGAGUCCUA-3′, 5′-GCGAGCUGAUGUAGAAUUA-3′, 5′-GGGA AUACAACUCCAAAUA-3′; *PTEN* SH-003023-01-10 5′-GCTAAGAGAGGT TTCCGAA-3′, SH-003023-02-10 5′-AGACTGATGTGTATACGTA-3′.

40. Lukacs, R. U., Goldstein, A. S., Lawson, D. A., Cheng, D. & Witte, O. N. Isolation, cultivation and characterization of adult murine prostate stem cells. *Nature Protocols* **5,** 702–713 (2010).
41. Lawson, D. A., Zong, Y., Memarzadeh, S., Xin, L., Huang, J. & Witte, O. N. Basal epithelial stem cells are efficient targets for prostate cancer initiation. *Proc. Natl Acad. Sci. USA* **107,** 2610–2615 (2010).

British Journal of Cancer (2011), 1 – 8

www.bjcancer.com

Minireview

Oncogenic AKTivation of translation as a therapeutic target

AC Hsieh[1,2], ML Truitt[1] and D Ruggero*[,1]

[1]Department of Urology, School of Medicine, Helen Diller Family Comprehensive Cancer Center, University of California, San Francisco, Helen Diller Family Cancer Research Building, Room 386, 1450 3rd Street, San Francisco, CA 94158-3110, USA; [2]Division of Hematology/Oncology, University of California, San Francisco, Helen Diller Family Cancer Research Building, Room 386, 1450 3rd Street, San Francisco, CA 94158-3110, USA

The AKT signalling pathway is a major regulator of protein synthesis that impinges on multiple cellular processes frequently altered in cancer, such as proliferation, cell growth, survival, and angiogenesis. AKT controls protein synthesis by regulating the multistep process of mRNA translation at every stage from ribosome biogenesis to translation initiation and elongation. Recent studies have highlighted the ability of oncogenic AKT to drive cellular transformation by altering gene expression at the translational level. Oncogenic AKT signalling leads to both global changes in protein synthesis as well as specific changes in the translation of select mRNAs. New and developing technologies are significantly advancing our ability to identify and functionally group these translationally controlled mRNAs into gene networks based on their modes of regulation. How oncogenic AKT activates ribosome biogenesis, translation initiation, and translational elongation to regulate these translational networks is an ongoing area of research. Currently, the majority of therapeutics targeting translational control are focused on blocking translation initiation through inhibition of eIF4E hyperactivity. However, it will be important to determine whether combined inhibition of ribosome biogenesis, translation initiation, and translation elongation can demonstrate improved therapeutic efficacy in tumours driven by oncogenic AKT.
British Journal of Cancer advance online publication, 19 July 2011; doi:10.1038/bjc.2011.241 www.bjcancer.com

Keywords: AKT; eIF4E; translational control; ribosome; PI3K; mTOR

TRANSLATIONAL CONTROL BY AKT

Protein synthesis is one of the most costly and tightly regulated energetic investments downstream of AKT signalling. AKT regulates protein synthesis through the phosphorylation of multiple downstream targets that function together to control all stages of mRNA translation from ribosome biogenesis to translation initiation and elongation (Figure 1). Ribosome biogenesis, translation initiation, and translation elongation are all frequently deregulated in cancer, and it is likely that oncogenic AKT drives tumour development and progression in part through its ability to coordinately activate these various steps of the translational process.

AKT activates translation initiation

One of the most rapid ways that AKT signalling enhances protein synthesis is through the activation of translation initiation. Translation initiation is the process by which ribosomes are recruited to the 5′ untranslated region (5′ UTR) of mature mRNAs in the first step of protein synthesis. In this process, 40S ribosomal subunits are recruited to the 7-methyl guanosine cap (5′ cap) of mRNAs by the eIF4F translation initiation complex through interactions with eukaryotic initiation factor 3 (eIF3; Emanuilov *et al*, 1978). eIF4F is a trimeric complex that resides at the cap. It is composed of the 5′ cap mRNA-binding protein eIF4E, the RNA helicase eIF4A, and the scaffolding molecule eIF4G (Haghighat and Sonenberg, 1997; Rogers *et al*, 1999). The majority of mRNA translation begins through eIF4F association with the cap and is known as cap-dependent translation. Translation initiation is considered to be the rate-limiting step of cap-dependent translation. eIF4E is considered as the key factor in controlling this step (Duncan *et al*, 1987). This thought is based largely on the fact that eIF4E activity is highly regulated at both the mRNA and protein level. eIF4E is upregulated at the mRNA level by a number of transcription factors including the oncogene MYC (Jones *et al*, 1996). At the protein level, eIF4E activity is controlled through an activating phosphorylation at serine 209, as well as through inhibitory interactions with the eIF4E-binding proteins (4EBPs; Gingras *et al*, 1998; Topisirovic *et al*, 2004). This tight regulation of eIF4E activity provides a rapid mechanism for cells to modulate translation initiation in response to numerous stimuli, including growth factor and oncogenic signalling.

AKT controls translation initiation largely through activation of the kinase mammalian target of rapamycin complex 1 (mTORC1). mTORC1 phosphorylates ribosomal protein (RP) S6 kinase 1/2 (S6K1/2) and the 4EBPs (Brown *et al*, 1995; von Manteuffel *et al*, 1997; Gingras *et al*, 1998). The 4EBPs are a family of small proteins (4EBP1 – 3) that compete with eIF4G for binding to the dorsal surface of eIF4E. In a hypophosphorylated state, 4EBPs prevent the formation of the eIF4F complex on the 5′ UTR of mRNAs by binding to eIF4E and preventing eIF4G recruitment (Figure 2). However, on growth factor stimulation, 4EBPs are phosphorylated at multiple serine/threonine residues in a series initiated by mTORC1 (Gingras *et al*, 1999, 2001). This leads to a conformational change that releases 4EBPs from eIF4E and allows eIF4G to bind eIF4E and ultimately recruit the 40S ribosomal subunit to the 5′ end of mRNAs. As a result, eIF4E regulates global protein synthesis by controlling the rate that ribosomes are able to dock onto the 5′ cap of mRNAs.

*Correspondence: Dr D Ruggero; E-mail: Davide.Ruggero@ucsf.edu
Received 16 February 2011; revised 1 June 2011; accepted 7 June 2011

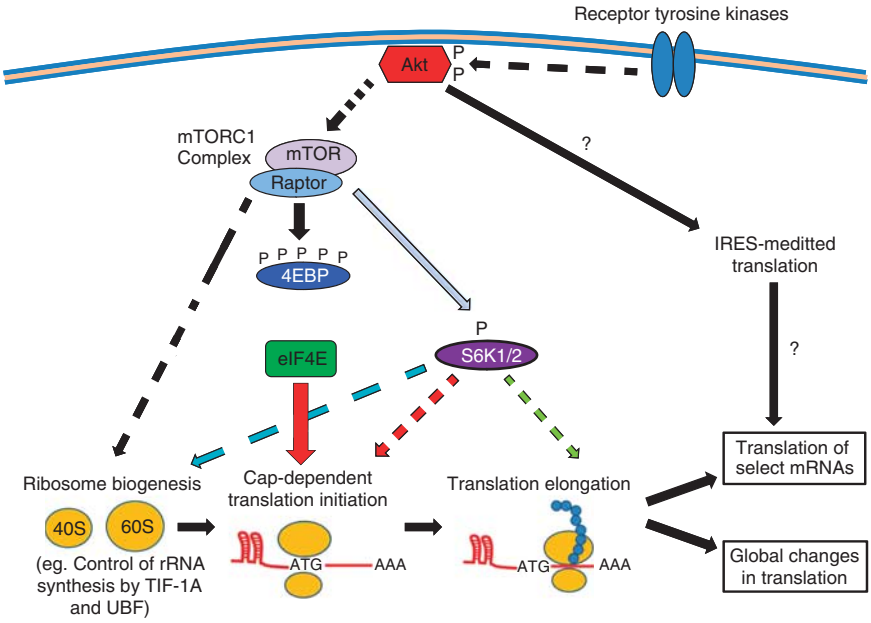

Figure 1 AKT signalling coordinately regulates translation. AKT is activated downstream of various cellular and oncogenic stimuli, such as receptor tyrosine kinase (RTK) signalling, to promote protein synthesis. AKT may accomplish this through coordinated regulation of ribosome biogenesis, translation initiation, and translation elongation. AKT-driven protein synthesis requires a full repertoire of mature ribosomes, and AKT has been shown to promote ribosome biogenesis through both enhanced rRNA synthesis and enhanced ribosomal protein production. In addition, AKT promotes protein synthesis through the activation of translation initiation factors that drive cap-dependent translation. This is one of the most rapid mechanisms by which AKT can activate protein synthesis, and it occurs largely through mTORC1-dependent phosphorylation of the 4EBPs. Furthermore, AKT has been shown to affect the efficiency of translation through the control of translation elongation factors. Translation can also be regulated through additional mechanisms, such as IRES-mediated translation, and it remains to be seen what effect AKT signalling may have on these processes. Together, AKT regulates the multiple stages of translation to drive both global changes in protein synthesis as well as selective changes in the translation of specific mRNAs.

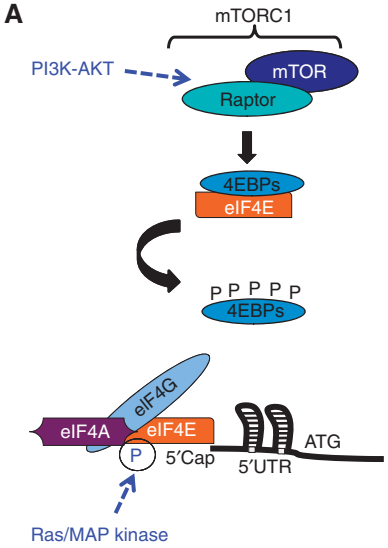

B

Therapeutic	Target	Status
eIF4E ASO	eIF4E mRNA	Phase I/II
4EGI-1	eIF4E interaction with eIF4G	Preclinical
Ribavirin	eIF4E cap binding	Phase II
Mnk 1/2 inhibitors	eIF4E phosphorylation	Preclinical
mTOR ATP-active site inhibitors	mTORC1-dependent 4EBP phosphorylation	Phase I

Figure 2 Targeting eIF4E hyperactivation in cancer. (**A**) Oncogenic AKT signalling promotes translation initiation predominantly through mTORC1-dependent hyperactivation of eIF4E. In the absence of signalling, hypophosphorylated 4EBP binds to and inhibits eIF4E, blocking its ability to interact with eIF4G. AKT signalling activates mTORC1, initiating a series of phosphorylations that release 4EBP from eIF4E. This allows for eIF4G binding to eIF4E and the subsequent recruitment of the 40S ribosomal subunit. In addition, it has been shown that Ras/MAP kinase signalling can promote eIF4E hyperactivation through downstream phosphorylation of eIF4E at Serine 209. (**B**) Current clinical status and proposed mechanistic targets of therapeutics designed to inhibit eIF4E hyperactivation in cancer.

In addition to global increases in protein synthesis, eIF4E hyperactivation is able to enhance the translation of select mRNAs (Mamane *et al*, 2007). The 5′ UTR of these mRNAs are believed to be the regulatory factors that impart this selectivity. 5′ UTRs can vary in length and GC nucleotide content, resulting in a range of secondary mRNA structures. These structures function as physical

barriers that limit the ability of the 40S ribosome to reach the translation start site (Manzella and Blackshear, 1990). As such, mRNAs with complex 5′ UTRs have low basal rates of translation and are exquisitely sensitive to eIF4E hyperactivation due to the ability of eIF4E to recruit the eIF4A helicase. eIF4A recruitment allows for enhanced unwinding of secondary structures in the 5′ UTR, resulting in improved translation initiation efficiency. Genes that are sensitive to eIF4E-mediated translation cover a range of cellular functions, including cell cycle control (cyclin D1), angiogenesis (VEGF), metabolism (ODC), and apoptosis (survivin and Mcl-1) among others (Rousseau *et al*, 1996; Graff *et al*, 2007; Mamane *et al*, 2007; Mills *et al*, 2008).

Despite the identification of mRNA targets that rely on the eIF4F complex for efficient translation (see above), several unbiased screens have also identified transcripts that lack complex 5′ UTRs, but are sensitive to eIF4E hyperactivation (Larsson *et al*, 2006; Mamane *et al*, 2007). One such class of genes is the 5′ TOP genes. 5′ TOP genes (terminal oligopyrimidine or tract of oligopyrimidine genes) are characterised by oligopyrimidine repeats in the 5′ UTR and predominantly encode for RPs, translation initiation factors, and translation elongation factors (Levy *et al*, 1991; Avni *et al*, 1994, 1997). While it is still unknown how hyperactivated eIF4E specifically regulates the translation of 5′ TOP genes, the fact that these genes do not possess complex 5′ UTRs suggests that there are other mechanisms of translational regulation downstream of eIF4E that have not been described. How might these additional regulatory mechanisms occur? One possible mechanism by which eIF4E could regulate translation is through direct interaction with inhibitory mRNA secondary structures outside of the 5′ UTR. eIF4E hyperactivation could promote unwinding of these structures through the recruitment of the eIF4A helicase, allowing for mRNA translation. In support of this, it was recently shown that eIF4E binds to a specific secondary structure outside of the 5′ UTR of Histone H4 mRNA to promote the translation of this mRNA in an eIF4A-dependent manner (Martin *et al*, 2011).

To elucidate how unique mRNA secondary structures interact with the translation initiation complex and the scanning ribosome, it will require the development of techniques to determine simultaneously the position of ribosomes on mRNAs and the precise secondary structures at that particular location. There are now rising technologies that may allow for this. In particular, the ability to deep-sequence ribosome-protected mRNAs has enabled us to determine the precise location of actively translating ribosomes (Ingolia *et al*, 2009). Furthermore, through deep sequencing, it is also now possible to determine the secondary structures of mRNAs by using parallel analysis of secondary structures (Kertesz *et al*, 2010). The combination of these two technologies may provide a very accurate portrait of how mRNA secondary structures control cap-dependent translation and allow for the identification of translational networks of genes with common regulatory elements within their mRNAs.

AKT promotes translation elongation

Although significant attention has been focused on the ability of AKT to regulate translation initiation, evidence suggests that other steps of translation, such as translation elongation, are also regulated by AKT signalling. Translation elongation is the process by which amino acid-charged tRNAs dock onto the ribosome/mRNA complex and incorporate amino acids into the growing nascent polypeptide chain. Multiple elongation factors are necessary to carry out this process efficiently. The eukaryotic translation elongation factor 2 (eEF2) mediates the translocation step of elongation, where tRNAs move between the P and A site on the ribosome as the ribosome migrates by one codon along the mRNA. AKT can promote this elongation step through S6K1/2-dependent inhibition of eEF2 kinase, a negative regulator of eEF2 (Wang *et al*, 2001). Thus, AKT activation not only affects translation initiation but also the efficiency of actively translating ribosomes. In addition, there is evidence that AKT activation may more broadly impact translation elongation through the preferential translation of 5′ TOP genes (see above), many of which encode for translation elongation factors (Avni *et al*, 1997; Mamane *et al*, 2007). While many mechanistic gaps still exist, it will be important to understand the degree to which AKT-activated translation elongation can enhance protein synthesis. Furthermore, it needs to be established if this ability of AKT to modulate translation elongation can contribute to AKT-driven tumourigenesis. It is interesting to speculate that oncogenic AKT may promote translation elongation not to cause increases in global protein synthesis but to instead preferentially promote the translation of select mRNAs.

AKT controls ribosome biogenesis

Protein synthesis depends on the generation of properly assembled, mature ribosomes. The biogenesis of mature ribosomes involves the synthesis and processing of rRNA, the synthesis of RPs, and the proper assembly of all these components within the nucleolus. AKT has been shown to modulate various aspects of these processes predominantly through mTOR activation. For example, mTOR can enhance the transcription of rDNA through activation of transcription initiation factor 1A (TIF-1A), a RNA polymerase I (Pol I) transcription factor. Through an indirect mechanism, mTOR simultaneously promotes an activating phosphorylation and blocks an inhibitory phosphorylation of TIF-1A to enhance rRNA synthesis (Mayer *et al*, 2004). In addition, mTOR can promote rRNA synthesis through activation of another Pol I transcription factor, upstream binding factor (UBF). Although the precise mechanism behind mTOR-dependent UBF activation has not been identified, S6K1 is thought to be required for UBF activation (Hannan *et al*, 2003). While AKT has been shown to enhance rRNA synthesis through multiple mechanisms, the ability of AKT to regulate other ribosomal constituents is less well defined. AKT activation may promote RP synthesis through enhanced translation of 5′ TOP genes (see above), which include many RPs. In addition, it has been demonstrated in yeast that RP synthesis is positively regulated by mTOR. In this setting, mTOR promotes the transcription of RP genes by indirectly activating transcription factors such as FHL1 (Martin *et al*, 2004). Despite evidence that AKT signalling can regulate ribosomal biogenesis through modulation of both rRNA synthesis and RP synthesis, the connection between ribosomal biogenesis and protein synthesis remains poorly defined. While studies have shown that normal ribosomal biogenesis is in fact required for protein synthesis, it is not clear if enhanced ribosomal biogenesis is able to drive increased protein synthesis downstream of oncogenic AKT.

AKT and IRES-mediated translation

Another mechanism of initiating translation, which may be targeted by AKT, is internal ribosome entry site (IRES)-mediated translation. IRES elements are mRNA secondary structures predominantly located within the 5′ UTR (and to a lesser extent in the coding sequence and intronic regions of mRNA) that can associate with IRES *trans*-acting factors (ITAFs) to initiate translation in a 5′ cap and eIF4E-independent manner. Only a subset of mRNAs contains IRES sequences. Thus, IRES-mediated translation is thought to be a fine-tuning mechanism that controls the translation of key mRNAs under specific physiological conditions such as the G0/quiescent and G2/M phases of the cell cycle, where it modulates proliferation, as well as under specific stress conditions such as hypoxia, where it promotes cell survival and angiogenesis (Pyronnet *et al*, 2000; Miskimins *et al*, 2001; Kullmann *et al*, 2002; Braunstein *et al*, 2007). IRES-mediated translation has been shown to have a role in cancer. One example

for this is in the setting of hypoxia in invasive breast cancer, where it has been demonstrated in a mouse model that eIF4E-mediated translation is downregulated through increased expression of 4EBP1 under hypoxic conditions. Despite a resulting decrease in overall protein synthesis levels, specific IRES containing mRNAs such as VEGF, HIF-1α, and Bcl-2 are translated at higher rates, thereby increasing the protein levels of these protumourigenic targets (Braunstein *et al*, 2007). In this manner, IRES-mediated translation enhances survival under specific cellular conditions.

Recently, there has been intriguing evidence that AKT may regulate IRES-mediated translation at the level of ITAFs. In particular, AKT was shown to directly phosphorylate the ITAF hnHRP1A at serine 199 and inhibit IRES-mediated translation (Jo *et al*, 2008). In this way, AKT may actively limit IRES-mediated translation through phosphorylation of ITAFs while it simultaneously promotes cap-dependent translation (see above). Further studies will be needed to delineate the role that inhibition of IRES-mediated translation has in AKT-driven tumour development and progression.

AKT signalling functions as a critical node for mRNA translation, coordinating everything from ribosome biogenesis to translation initiation and elongation. AKT collectively activates these stages of translational control to drive increased cellular protein synthesis. Despite strong evidence that AKT signalling can regulate ribosome biogenesis, translation initiation, and translation elongation, we still do not understand the relative role that these events have in AKT-induced protein synthesis. Future studies will be needed to determine the extent to which activation of these translational steps, either alone or in combination, is sufficient to drive protein synthesis. In addition, it will be important to understand the requirement for activation of each of these translational stages in tumours driven by oncogenic AKT signalling. Despite the fact that AKT functions as a master regulator of translational control through mTOR activation, AKT also has other well-characterised targets, including but not limited to FOXO, GSK3, and MDM2, which control diverse cellular processes, such as cell survival, proliferation, and angiogenesis, without directly impinging on mRNA translation (Manning and Cantley, 2007). For example, AKT-mediated phosphorylation and activation of MDM2 leads to p53 ubiquitination, degradation, and significantly impairs the cellular DNA damage response (Zhou *et al*, 2001). Thus, oncogenic AKT exhibits its transforming potential through multiple mechanisms. Intriguingly, several downstream effectors of mTOR-independent AKT targets have been shown to be translationally regulated. For example, AKT promotes cell survival in part through inhibition of GSK3, preventing the phosphorylation and subsequent degradation of the prosurvival Bcl-2 family member Mcl-1 (Maurer *et al*, 2006), and Mcl-1 has also been shown to be translationally upregulated downstream of oncogenic AKT signalling (Hsieh *et al*, 2010). Therefore, it remains an open and outstanding question to what extent AKT-mediated translational control cooperates with key non-mTOR-dependent AKT substrates to regulate critical cellular events to promote tumourigenesis and cancer progression.

TRANSLATION INITIATION IS CRITICALLY REQUIRED FOR ONCOGENIC AKT ACTIVITY

The AKT signalling pathway is heavily mutated in a variety of human malignancies. In fact, mutations of AKT pathway components and upstream regulators cover nearly the entire spectrum of human cancers, suggesting a broad requirement for AKT activation in tumourigenesis (Table 1). Although genetic alterations of AKT are relatively rare in human cancers, multiple mouse studies have demonstrated that the expression of constitutively active AKT isoforms is sufficient to drive tumourigenesis (Mende *et al*, 2001; Majumder *et al*, 2003; Tan *et al*, 2008). Furthermore, AKT hyperactivity has been shown to be critically required for tumourigenesis caused by more frequently occurring genetic lesions upstream of AKT signalling, such as PTEN loss (Chen *et al*, 2006). Despite a wealth of knowledge on genetic mutations leading to the oncogenic activation of AKT and a growing appreciation for the ability of AKT to coordinately regulate mRNA translation, the extent to which deregulated AKT

Table 1 Common mutations in the PI3K–AKT–mTOR signalling pathway

Targets	Genetic alteration	Cancer type
PIK3CA (phosphoinositide-3-kinase, catalytic, α-polypeptide)	Mutations	Breast, endometrial, colon, upper digestive tract, gastric, pancreas, ovarian, liver, brain, oesophageal, lung, melanoma, urinary tract, prostate, thyroid
	Amplifications	Lung (squamous cell), lung (adenocarcinoma), lung (small cell), lung (non-small cell), cervical, breast, head and neck, gastric, thyroid, oesophageal, endometrial, ovarian, glioblastoma
PIK3CB (phosphoinositide-3-kinase, catalytic, β-polypeptide)	Amplifications	Ovarian, breast
	Increase in activity and expression	Colon, bladder
PDPK1 (3-phosphoinositide dependent protein kinase-1)	Amplifications and overexpression	Breast
AKT (v-akt murine thymoma viral oncogene homologue)	AKT homologue 1 mutation (E17K) or amplifications	Breast, colon, ovarian, lung, gastric
	AKT homologue 2 amplifications	Ovarian, pancreas, head and neck, breast
	AKT homologue 3 mutation (E17K) or amplifications	Skin, glioblastoma
PIK3R1 (phosphoinositide-3-kinase, regulatory subunit-1)	Mutations	Glioblastoma, ovarian, colon
PTEN (phosphatase and tensin homologue)	Loss of heterozygosity	Gastric, breast, melanoma, prostate, glioblastoma
	Mutations	Endometrial, brain, skin, prostate, colon, ovary, breast, haematopoietic and lymphoid tissue, stomach, liver, kidney, vulva, urinary tract, thyroid, lung

translational control functions as an oncogenic driver remains largely undefined. Recent studies have, however, highlighted a critical requirement for enhanced translation initiation downstream of oncogenic AKT signalling. Strikingly, oncogenic AKT seems to enhance translation initiation largely through hyperactivation of the eIF4E translation initiation factor, which is a bona-fide oncogene.

The oncogenic potential of eIF4E has been well described both *in vitro* and *in vivo*. Overexpression of eIF4E is sufficient to induce transformation of fibroblasts and primary epithelial cells in culture, and eIF4E overexpression in mice leads to increased cancer susceptibility in a range of tissues (Lazaris-Karatzas *et al*, 1990; Avdulov *et al*, 2004; Ruggero *et al*, 2004). While these findings, along with evidence of eIF4E overexpression in human cancers (Flowers *et al*, 2009; Graff *et al*, 2009; Wang *et al*, 2009), support the notion that eIF4E is oncogenic, a direct connection between eIF4E and translational deregulation downstream of oncogenic AKT signalling has only recently been described. Some of the first evidence for such a connection came from a study showing that pharmacological inhibition of oncogenic RAS and AKT in glioblastoma cells caused a rapid and profound change in mRNA translation that far outweighed transcriptional changes and was associated with loss of mTORC1-dependent phosphorylation of 4EBPs (Rajasekhar *et al*, 2003). This study identified translational regulation of several mRNA targets important for cancer development, and suggested that altered translational control downstream of eIF4E hyperactivation may be required for AKT-driven cellular transformation.

Our group demonstrated *in vivo* that hyperactivation of eIF4E is necessary for AKT-mediated tumourigenesis. Using a T-cell lymphoma model driven by overexpression of constitutively active AKT, we showed that enhanced protein synthesis through eIF4E hyperactivation was required for AKT-mediated tumourigenesis. We found that AKT overexpressing pretumour progenitor T cells possessed a distinct survival advantage, which was abrogated when eIF4E hyperactivity was restored to wild-type levels. Using a candidate gene approach, we found that this survival advantage was due in part to translational upregulation of the antiapoptotic Mcl-1. Importantly, we were also able to pharmacologically inhibit eIF4E hyperactivity downstream of oncogenic AKT, which resulted in significant inhibition of tumour growth (see below; Hsieh *et al*, 2010). As such, we identified the 4EBP/eIF4E axis as a druggable target that regulates translation downstream of oncogenic AKT.

The requirement for eIF4E hyperactivity in AKT-driven tumours has been further substantiated by recent studies. For example, it was found that the efficacy of an AKT inhibitor in human cancer cell lines correlated with its ability to inhibit phosphorylation of 4EBPs and block cap-dependent translation. This study showed that in cell lines where AKT inhibition failed to block phosphorylation of 4EBPs, the MAPK signalling pathway was frequently activated. The authors further demonstrated that combined pharmacological inhibition of AKT and MAPK signalling was able to inhibit phosphorylation of 4EBPs and prevent the *in vivo* growth of cell lines resistant to AKT inhibition alone. Importantly, the authors were able to attribute this combinatorial drug effect directly to the inhibition of eIF4E hyperactivity, as the overexpression of a non-phosphorylatable form of 4EBP1 was sufficient to block the growth of these cells in xenografts (She *et al*, 2010).

In addition to 4EBP-dependent control, eIF4E activity is positively regulated through phosphorylation at serine 209 by the MAP kinase targets MNK1/2. Whole body expression of a knock-in mutant of eIF4E, which can no longer be phosphorylated at this residue, was found to decrease the incidence and grade of prostatic intraepithelial neoplasia in a mouse prostate cancer model driven by PTEN loss (Furic *et al*, 2010). While this study supports a role for eIF4E hyperactivation downstream of oncogenic AKT signalling, it raises several questions: Do all tissues rely on phosphorylation of serine 209 for hyperactivation of eIF4E downstream of oncogenic AKT signalling? More broadly, what is the tissue-specific dependence of eIF4E hyperactivation, which could be achieved by different mechanisms, downstream of oncogenic AKT? Indeed, there is convincing genetic evidence that oncogenic eIF4E alone is sufficient to drive tumourigenesis in specific tissues. Transgenic mice that ubiquitously overexpress eIF4E show that distinct tissues, including the lungs, liver, and the lymphoid compartment, are more prone to oncogenic transformation (Ruggero *et al*, 2004). As such, we can speculate that there may be tissue-specific requirements for the eIF4E oncogenic activity downstream of AKT hyperactivation in tumour development. Although many important questions remain to be addressed, the above studies show that eIF4E hyperactivation is not only critically required for AKT-driven tumours but it might also serve as a node on which multiple oncogenic signalling pathways converge, thus representing an attractive therapeutic target.

TARGETING EIF4E HYPERACTIVATION

Antisense targeting of eIF4E – eIF4E ASO

eIF4E is a bona-fide oncogene frequently hyperactivated downstream of oncogenic AKT signalling, and thus represents an attractive target for rational drug design. There are currently several approaches being pursued to therapeutically inhibit eIF4E, but perhaps the most direct of these approaches is the use of specific antisense oligonucleotides (ASOs) that bind to eIF4E mRNA and mediate its destruction by RNase H. Nanomolar concentrations of eIF4E ASOs have been shown to decrease eIF4E protein levels in several human cancer cell lines *in vitro*, reducing protein levels of known eIF4E targets and inducing apoptosis. In tumour xenograft models, eIF4E ASOs inhibited tumour growth without any detectable changes in body weight or liver function. Strikingly, control mice treated with eIF4E ASOs for 3 weeks showed no signs of toxicity, despite reductions in eIF4E protein levels by up to 80% in the liver, implying a critical difference in the requirement of eIF4E for normal physiological function (Graff *et al*, 2007). These studies suggest that tumours may be sensitive to eIF4E inhibition while normal tissues are not, but for what duration and to what extent eIF4E can be inhibited system-wide without detriment remains an open question.

eIF4E–eIF4G interaction inhibitor – 4EGI-1

Additional attempts to target eIF4E have focused on blocking its ability to interact with eIF4G. The interaction between eIF4E and eIF4G is dependent on an eIF4G $Y(X)_4L\Phi$ motif, where X is variable and Φ is hydrophobic (Altmann *et al*, 1997). High-throughput screens for inhibitors that could prevent eIF4E binding to the $Y(X)_4L\Phi$ motif identified 4EGI-1 as a candidate compound. 4EGI-1 was able to inhibit eIF4F complex formation at micromolar concentrations. Surprisingly, 4EGI-1 did not block the ability of eIF4E to bind to 4EBP1, which, similar to eIF4G, contains a $Y(X)_4L\Phi$ motif. 4EGI-1 was shown to be cytostatic and cytotoxic in multiple cell lines and preferentially blocked the growth of transformed cells over untransformed cells (Moerke *et al*, 2007). Recently, it has been reported that 4EGI-1 functions through an eIF4G/eIF4E-independent mechanism to promote apoptosis in human lung cancer cells (Fan *et al*, 2010). Additionally, 4EGI-1 has been shown to suppress translation in primary human cells at concentrations below those required for eIF4E inhibition (McMahon *et al*, 2011). Collectively, these studies suggest that 4EGI-1 may have antitumour efficacy through more general inhibition of oncogenic pathways and that the full spectrum of protein–protein interactions and pathways that 4EGI-1 blocks still needs to be determined. Despite these concerns, specifically targeting the

eIF4E/eIF4G protein–protein interaction is an attractive therapeutic approach, and subsequent generations of such inhibitors may provide a novel and important way of targeting eIF4E in human cancers.

Targeting the eIF4E-5′ cap interaction – Ribavirin

eIF4E function can also be directly inhibited by blocking its ability to interact with the 5′ cap of mRNAs. Ribavirin, a guanosine ribonucleoside currently used as an anti-viral therapy, has recently been shown to compete with endogenous mRNAs for binding to eIF4E, leading to decreased eIF4F complex formation *in vitro*. In line with this, ribavirin blocked eIF4E-mediated oncogenic transformation *in vitro* and demonstrated *in vivo* efficacy in preclinical models of acute myelogenous leukaemia (AML) and squamous cell carcinoma (Kentsis *et al*, 2004). In a phase I dose-escalation trial with ribavirin, 7 out of 11 AML patients were reported to have at least partial responses or stable disease (Assouline *et al*, 2009). Although ribavirin may ultimately prove to have clinical efficacy in human cancers, the specific function of ribavirin as a cap-mimetic has been called into question by two independent groups (Westman *et al*, 2005; Yan *et al*, 2005). Therefore, it is not clear if the inhibition of cap-dependent translation underlies ribavirin's therapeutic efficacy.

Inhibition of eIF4E phosphorylation – MNK kinase inhibitors

The MNK kinases are activated downstream of MAP kinase signalling and directly phosphorylate eIF4E at serine 209 (Scheper *et al*, 2001). Mutation of eIF4E at this residue blocks its transforming potential *in vitro* and can inhibit PTEN-driven tumourigenesis *in vivo* (Furic *et al*, 2010). Furthermore, mice doubly deficient for MNK1 and MNK2 are resistant to lymphomagenesis driven by PTEN loss, validating the MNKs as potential therapeutic targets upstream of eIF4E (Ueda *et al*, 2010). Recently, a high-throughput screen identified the antifungal cercosporamide as a potent inhibitor of MNK1 and MNK2 with limited activity towards other kinases. Cercosporamide was able to block eIF4E phoshorylation *in vivo* and inhibit the growth of human xenografts as well as the metastasis of mouse melanoma cells (Konicek *et al*, 2011). Although these results are promising and suggest that targeted inhibition of eIF4E phosphorylation may be a valid therapeutic approach, it remains unclear to what extent the efficacy of MNK kinase inhibitors can be attributed to their ability to block other downstream phosphorylation targets critical for tumour growth and maintenance. Regardless, the observation that both MNK kinase activity and eIF4E phosphorylation are dispensable for normal growth and development, but are required for tumourigenesis, makes the MNK kinases attractive therapeutic targets.

mTOR ATP active-site inhibitors

Perhaps one of the most promising approaches to therapeutically block eIF4E hyperactivity is the targeted inhibition of the mTOR kinase. First-generation allosteric mTOR inhibitors such as rapamycin, RAD001, and CCI-779 inconsistently inhibit phosphorylation of 4EBP1 downstream of mTORC1, despite potently inhibiting S6K phosphorylation (Choo *et al*, 2008; Hsieh *et al*, 2010). This suggests that phosphorylation of S6K or its downstream target rpS6 may not serve as an accurate readout for inhibition of all mTORC1 kinase activity. Indeed, the poor clinical performance of rapamycin and its associated analogues in human cancer is most likely due to their inability to block mTORC1-dependent phosphorylation of 4EBPs and thus fully inhibit eIF4E activation (see above). In order to overcome the incomplete inhibition seen with allosteric mTOR inhibitors, our group and several others have identified mTOR ATP active-site inhibitors, such as PP242 and Torin1 (Feldman *et al*, 2009; Thoreen *et al*, 2009). These compounds reversibly compete with ATP for binding to the mTOR catalytic domain and thus block not only mTORC1 activity, but also mTORC2 activity. mTORC2, an mTOR complex distinct from mTORC1, is responsible for an activating phosphorylation of AKT at Serine 473. Using PP242, our group was the first to demonstrate that these ATP active-site inhibitors effectively inhibit phosphorylation of the 4EBPs, the S6Ks, and AKT. This is in striking contrast to rapamycin, which predominantly blocks the phosphorylation of S6Ks and infrequently blocks the phosphorylation of 4EBPs. As a result, PP242 inhibits the proliferation of cultured cell lines to a much greater extent than rapamycin. Furthermore, our group has shown that PP242 dramatically inhibits tumour growth in an AKT-driven mouse model of lymphoma that is inherently resistant to rapamycin. Strikingly, tumours from the same model that overexpressed a mutated non-phosphorylatable 4EBP1 transgene were completely insensitive to PP242 inhibition, suggesting that PP242 efficacy may be entirely due to its ability to block mTORC1-dependent 4EBP phosphorylation (Hsieh *et al*, 2010). In line with this, PP242 and Torin1 both retain their antiproliferative effects in mouse embryonic fibroblasts, in which the mTORC2 complex has been destabilised (Feldman *et al*, 2009; Thoreen *et al*, 2009). Although these studies suggest that the antitumour effect of mTOR ATP active-site inhibitors is predominantly mediated by blocking phosphorylation of 4EBPs and eIF4E hyperactivity, they cannot generally rule out a role for the inhibition of other translational regulators downstream of mTORC1. Furthermore, it remains to be seen how these ATP active-site inhibitors, which have been found to block growth of cell lines and murine lymphomas, will perform in solid human epithelial tumours.

FUTURE DIRECTIONS

Oncogenic AKT signalling utilises the multistep process of mRNA translation to drive tumour development and progression. Despite significant advances in our understanding of AKT-mediated translational control and the development of promising therapeutics to target deregulated translation initiation in human cancers, many questions and opportunities remain. Although AKT signalling has been shown to control the translational steps of ribosome biogenesis, translation initiation, and translation elongation, it is still an open question if oncogenic AKT requires the hyperactivation of all three translational steps for tumourigenesis and cancer progression. This is an important question because most preclinical and clinical studies to date have focused on targeting translation initiation downstream of oncogenic AKT. Recently, it has been shown that targeting ribosome biogenesis through pol I inhibition (CX-5461) or targeting various aspects of translation elongation leads to significant antitumour activity *in vivo* (Robert *et al*, 2009; Drygin *et al*, 2011). Thus, it will be important to determine whether more comprehensive inhibition of oncogenic AKT-driven translation through combined targeting of ribosome biogenesis, translation initiation, and translation elongation results in clinically significant improvements in patient survival. Attempts to target translational control downstream of oncogenic AKT will be further aided by the use of novel technologies and analyses to identify networks of translationally controlled genes that may function as critical biomarkers for disease progression and therapeutic response.

Finally, there is a growing body of evidence that deregulation of translational control may be a common mechanism by which oncogenic pathways promote tumour initiation and progression (e.g., MYC and RAS). As such, efforts to target translational control may prove successful in a wide array of human malignancies.

ACKNOWLEDGEMENTS

We thank Maria Barna and members of the Ruggero lab for input and critical reading of this review. We also thank Kimhouy Tong for editing the manuscript. We apologise to the many scientists whose work we were unable to cite. DR is a Leukemia & Lymphoma Society Scholar. ACH is a postdoctoral fellow of the American Cancer Society and a Prostate Cancer Foundation Young Investigator. This work is supported by NIH R01 HL085572 (DR) and NIH R01 CA140456 (DR).

REFERENCES

Altmann M, Schmitz N, Berset C, Trachsel H (1997) A novel inhibitor of cap-dependent translation initiation in yeast: p20 competes with eIF4G for binding to eIF4E. *EMBO J* **16:** 1114 – 1121

Assouline S, Culjkovic B, Cocolakis E, Rousseau C, Beslu N, Amri A, Caplan S, Leber B, Roy DC, Miller Jr WH, Borden KL (2009) Molecular targeting of the oncogene eIF4E in acute myeloid leukemia (AML): a proof-of-principle clinical trial with ribavirin. *Blood* **114:** 257 – 260

Avdulov S, Li S, Michalek V, Burrichter D, Peterson M, Perlman DM, Manivel JC, Sonenberg N, Yee D, Bitterman PB, Polunovsky VA (2004) Activation of translation complex eIF4F is essential for the genesis and maintenance of the malignant phenotype in human mammary epithelial cells. *Cancer Cell* **5:** 553 – 563

Avni D, Biberman Y, Meyuhas O (1997) The 5′ terminal oligopyrimidine tract confers translational control on TOP mRNAs in a cell type- and sequence context-dependent manner. *Nucleic Acids Res* **25:** 995 – 1001

Avni D, Shama S, Loreni F, Meyuhas O (1994) Vertebrate mRNAs with a 5′-terminal pyrimidine tract are candidates for translational repression in quiescent cells: characterization of the translational cis-regulatory element. *Mol Cell Biol* **14:** 3822 – 3833

Braunstein S, Karpisheva K, Pola C, Goldberg J, Hochman T, Yee H, Cangiarella J, Arju R, Formenti SC, Schneider RJ (2007) A hypoxia-controlled cap-dependent to cap-independent translation switch in breast cancer. *Mol Cell* **28:** 501 – 512

Brown EJ, Beal PA, Keith CT, Chen J, Shin TB, Schreiber SL (1995) Control of p70 s6 kinase by kinase activity of FRAP *in vivo*. *Nature* **377:** 441 – 446

Chen ML, Xu PZ, Peng XD, Chen WS, Guzman G, Yang X, Di Cristofano A, Pandolfi PP, Hay N (2006) The deficiency of Akt1 is sufficient to suppress tumor development in Pten+/− mice. *Genes Dev* **20:** 1569 – 1574

Choo AY, Yoon SO, Kim SG, Roux PP, Blenis J (2008) Rapamycin differentially inhibits S6Ks and 4E-BP1 to mediate cell-type-specific repression of mRNA translation. *Proc Natl Acad Sci USA* **105:** 17414 – 17419

Drygin D, Lin A, Bliesath J, Ho CB, O'Brien SE, Proffitt C, Omori M, Haddach M, Schwaebe MK, Siddiqui-Jain A, Streiner N, Quin JE, Sanij E, Bywater MJ, Hannan RD, Ryckman D, Anderes K, Rice WG (2011) Targeting RNA polymerase I with an oral small molecule CX-5461 inhibits ribosomal RNA synthesis and solid tumor growth. *Cancer Res* **71:** 1418 – 1430

Duncan R, Milburn SC, Hershey JW (1987) Regulated phosphorylation and low abundance of HeLa cell initiation factor eIF-4F suggest a role in translational control. Heat shock effects on eIF-4F. *J Biol Chem* **262:** 380 – 388

Emanuilov I, Sabatini DD, Lake JA, Freienstein C (1978) Localization of eukaryotic initiation factor 3 on native small ribosomal subunits. *Proc Natl Acad Sci USA* **75:** 1389 – 1393

Fan S, Li Y, Yue P, Khuri FR, Sun SY (2010) The eIF4E/eIF4G interaction inhibitor 4EGI-1 augments TRAIL-mediated apoptosis through c-FLIP Down-regulation and DR5 induction independent of inhibition of cap-dependent protein translation. *Neoplasia* **12:** 346 – 356

Feldman M, Apsel B, Uotila A, Loewith R, Knight Z, Ruggero D, Shokat K (2009) Active-site inhibitors of mTOR target rapamycin-resistant outputs of mTORC1 and mTORC2. *PLoS Biol* **7:** e38

Flowers A, Chu QD, Panu L, Meschonat C, Caldito G, Lowery-Nordberg M, Li BD (2009) Eukaryotic initiation factor 4E overexpression in triple-negative breast cancer predicts a worse outcome. *Surgery* **146:** 220 – 226

Furic L, Rong L, Larsson O, Koumakpayi IH, Yoshida K, Brueschke A, Petroulakis E, Robichaud N, Pollak M, Gaboury LA, Pandolfi PP, Saad F, Sonenberg N (2010) eIF4E phosphorylation promotes tumorigenesis and is associated with prostate cancer progression. *Proc Natl Acad Sci USA* **107:** 14134 – 14139

Gingras AC, Gygi SP, Raught B, Polakiewicz RD, Abraham RT, Hoekstra MF, Aebersold R, Sonenberg N (1999) Regulation of 4E-BP1 phosphorylation: a novel two-step mechanism. *Genes Dev* **13:** 1422 – 1437

Gingras AC, Kennedy SG, O'Leary MA, Sonenberg N, Hay N (1998) 4E-BP1, a repressor of mRNA translation, is phosphorylated and inactivated by the Akt(PKB) signaling pathway. *Genes Dev* **12:** 502 – 513

Gingras AC, Raught B, Gygi SP, Niedzwiecka A, Miron M, Burley SK, Polakiewicz RD, Wyslouch-Cieszynska A, Aebersold R, Sonenberg N (2001) Hierarchical phosphorylation of the translation inhibitor 4E-BP1. *Genes Dev* **15:** 2852 – 2864

Graff JR, Konicek BW, Lynch RL, Dumstorf CA, Dowless MS, McNulty AM, Parsons SH, Brail LH, Colligan BM, Koop JW, Hurst BM, Deddens JA, Neubauer BL, Stancato LF, Carter HW, Douglass LE, Carter JH (2009) eIF4E activation is commonly elevated in advanced human prostate cancers and significantly related to reduced patient survival. *Cancer Res* **69:** 3866 – 3873

Graff JR, Konicek BW, Vincent TM, Lynch RL, Monteith D, Weir SN, Schwier P, Capen A, Goode RL, Dowless MS, Chen Y, Zhang H, Sissons S, Cox K, McNulty AM, Parsons SH, Wang T, Sams L, Geeganage S, Douglass LE, Neubauer BL, Dean NM, Blanchard K, Shou J, Stancato LF, Carter JH, Marcusson EG (2007) Therapeutic suppression of translation initiation factor eIF4E expression reduces tumor growth without toxicity. *J Clin Invest* **117:** 2638 – 2648

Haghighat A, Sonenberg N (1997) eIF4G dramatically enhances the binding of eIF4E to the mRNA 5′-cap structure. *J Biol Chem* **272:** 21677 – 21680

Hannan KM, Brandenburger Y, Jenkins A, Sharkey K, Cavanaugh A, Rothblum L, Moss T, Poortinga G, McArthur GA, Pearson RB, Hannan RD (2003) mTOR-dependent regulation of ribosomal gene transcription requires S6K1 and is mediated by phosphorylation of the carboxy-terminal activation domain of the nucleolar transcription factor UBF. *Mol Cell Biol* **23:** 8862 – 8877

Hsieh AC, Costa M, Zollo O, Davis C, Feldman ME, Testa JR, Meyuhas O, Shokat KM, Ruggero D (2010) Genetic dissection of the oncogenic mTOR pathway reveals druggable addiction to translational control via 4EBP-eIF4E. *Cancer Cell* **17:** 249 – 261

Ingolia NT, Ghaemmaghami S, Newman JR, Weissman JS (2009) Genome-wide analysis *in vivo* of translation with nucleotide resolution using ribosome profiling. *Science (New York, NY)* **324:** 218 – 223

Jo OD, Martin J, Bernath A, Masri J, Lichtenstein A, Gera J (2008) Heterogeneous nuclear ribonucleoprotein A1 regulates cyclin D1 and c-myc internal ribosome entry site function through Akt signaling. *J Biol Chem* **283:** 23274 – 23287

Jones RM, Branda J, Johnston KA, Polymenis M, Gadd M, Rustgi A, Callanan L, Schmidt EV (1996) An essential E box in the promoter of the gene encoding the mRNA cap-binding protein (eukaryotic initiation factor 4E) is a target for activation by c-myc. *Mol Cell Biol* **16:** 4754 – 4764

Kentsis A, Topisirovic I, Culjkovic B, Shao L, Borden KL (2004) Ribavirin suppresses eIF4E-mediated oncogenic transformation by physical mimicry of the 7-methyl guanosine mRNA cap. *Proc Natl Acad Sci USA* **101:** 18105 – 18110

Kertesz M, Wan Y, Mazor E, Rinn JL, Nutter RC, Chang HY, Segal E (2010) Genome-wide measurement of RNA secondary structure in yeast. *Nature* **467:** 103 – 107

Konicek BW, Stephens JR, McNulty AM, Robichaud N, Peery RB, Dumstorf CA, Dowless MS, Iversen P, Parsons SH, Ellis KE, McCann DJ, Pelletier J, Furic L, Yingling JM, Stancato LF, Sonenberg N, Graff JR (2011) Therapeutic inhibition of MAP kinase interacting kinase blocks eukaryotic initiation factor 4E phosphorylation and suppresses outgrowth of experimental lung metastases. *Cancer Res* **71:** 1849 – 1857

Kullmann M, Gopfert U, Siewe B, Hengst L (2002) ELAV/Hu proteins inhibit p27 translation via an IRES element in the p27 5′UTR. *Genes Dev* **16:** 3087 – 3099

Larsson O, Perlman D, Fan D, Reilly C, Peterson M, Dahlgren C, Liang Z, Li S, Polunovsky V, Wahlestedt C, Bitterman P (2006) Apoptosis resistance downstream of eIF4E: posttranscriptional activation of an anti-apoptotic transcript carrying a consensus hairpin structure. *Nucleic Acids Research* **34:** 4375 – 4386

Lazaris-Karatzas A, Montine KS, Sonenberg N (1990) Malignant transformation by a eukaryotic initiation factor subunit that binds to mRNA 5′ cap. *Nature* **345:** 544 – 547

Levy S, Avni D, Hariharan N, Perry RP, Meyuhas O (1991) Oligopyrimidine tract at the 5′ end of mammalian ribosomal protein mRNAs is required

for their translational control. *Proceedings of the National Academy of Sciences of the United States of America* **88:** 3319 – 3323

Majumder PK, Yeh JJ, George DJ, Febbo PG, Kum J, Xue Q, Bikoff R, Ma H, Kantoff PW, Golub TR, Loda M, Sellers WR (2003) Prostate intraepithelial neoplasia induced by prostate restricted Akt activation: the MPAKT model. *Proceedings of the National Academy of Sciences of the United States of America* **100:** 7841 – 7846

Mamane Y, Petroulakis E, Martineau Y, Sato TA, Larsson O, Rajasekhar VK, Sonenberg N (2007) Epigenetic activation of a subset of mRNAs by eIF4E explains its effects on cell proliferation. *PLoS One* **2:** e242

Manning BD, Cantley LC (2007) AKT/PKB signaling: navigating downstream. *Cell* **129:** 1261 – 1274

Manzella JM, Blackshear PJ (1990) Regulation of rat ornithine decarboxylase mRNA translation by its 5′-untranslated region. *The Journal of Biological Chemistry* **265:** 11817 – 11822

Martin DE, Soulard A, Hall MN (2004) TOR regulates ribosomal protein gene expression via PKA and the Forkhead transcription factor FHL1. *Cell* **119:** 969 – 979

Martin F, Barends S, Jaeger S, Schaeffer L, Prongidi-Fix L, Eriani G (2011) Cap-assisted internal initiation of translation of histone h4. *Mol Cell* **41:** 197 – 209

Maurer U, Charvet C, Wagman AS, Dejardin E, Green DR (2006) Glycogen synthase kinase-3 regulates mitochondrial outer membrane permeabilization and apoptosis by destabilization of MCL-1. *Mol Cell* **21:** 749 – 760

Mayer C, Zhao J, Yuan X, Grummt I (2004) mTOR-dependent activation of the transcription factor TIF-IA links rRNA synthesis to nutrient availability. *Genes Dev* **18:** 423 – 434

McMahon R, Zaborowska I, Walsh D (2011) Noncytotoxic inhibition of viral infection through eIF4F-independent suppression of translation by 4EGi-1. *J Virol* **85:** 853 – 864

Mende I, Malstrom S, Tsichlis PN, Vogt PK, Aoki M (2001) Oncogenic transformation induced by membrane-targeted Akt2 and Akt3. *Oncogene* **20:** 4419 – 4423

Mills JR, Hippo Y, Robert F, Chen SM, Malina A, Lin CJ, Trojahn U, Wendel HG, Charest A, Bronson RT, Kogan SC, Nadon R, Housman DE, Lowe SW, Pelletier J (2008) mTORC1 promotes survival through translational control of Mcl-1. *Proc Natl Acad Sci USA* **105:** 10853 – 10858

Miskimins WK, Wang G, Hawkinson M, Miskimins R (2001) Control of cyclin-dependent kinase inhibitor p27 expression by cap-independent translation. *Mol Cell Biol* **21:** 4960 – 4967

Moerke NJ, Aktas H, Chen H, Cantel S, Reibarkh MY, Fahmy A, Gross JD, Degterev A, Yuan J, Chorev M, Halperin JA, Wagner G (2007) Small-molecule inhibition of the interaction between the translation initiation factors eIF4E and eIF4G. *Cell* **128:** 257 – 267

Pyronnet S, Pradayrol L, Sonenberg N (2000) A cell cycle-dependent internal ribosome entry site. *Mol Cell* **5:** 607 – 616

Rajasekhar VK, Viale A, Socci ND, Wiedmann M, Hu X, Holland E (2003) Oncogenic Ras and Akt signaling contribute to glioblastoma formation by differential recruitment of existing mRNAs to polysomes. *Mol Cell* **12:** 889 – 901

Robert F, Carrier M, Rawe S, Chen S, Lowe S, Pelletier J (2009) Altering chemosensitivity by modulating translation elongation. *PLoS One* **4:** e5428

Rogers Jr GW, Richter NJ, Merrick WC (1999) Biochemical and kinetic characterization of the RNA helicase activity of eukaryotic initiation factor 4A. *J Biol Chem* **274:** 12236 – 12244

Rousseau D, Kaspar R, Rosenwald I, Gehrke L, Sonenberg N (1996) Translation initiation of ornithine decarboxylase and nucleocytoplasmic transport of cyclin D1 mRNA are increased in cells overexpressing eukaryotic initiation factor 4E. *Proc Natl Acad Sci USA* **93:** 1065 – 1070

Ruggero D, Montanaro L, Ma L, Xu W, Londei P, Cordon-Cardo C, Pandolfi P (2004) The translation factor eIF-4E promotes tumor formation and cooperates with c-Myc in lymphomagenesis. *Nat Med* **10:** 484 – 486

Scheper GC, Morrice NA, Kleijn M, Proud CG (2001) The mitogen-activated protein kinase signal-integrating kinase Mnk2 is a eukaryotic initiation factor 4E kinase with high levels of basal activity in mammalian cells. *Mol Cell Biol* **21:** 743 – 754

She QB, Halilovic E, Ye Q, Zhen W, Shirasawa S, Sasazuki T, Solit DB, Rosen N (2010) 4E-BP1 is a key effector of the oncogenic activation of the AKT and ERK signaling pathways that integrates their function in tumors. *Cancer Cell* **18:** 39 – 51

Tan Y, Timakhov RA, Rao M, Altomare DA, Xu J, Liu Z, Gao Q, Jhanwar SC, Di Cristofano A, Wiest DL, Knepper JE, Testa JR (2008) A novel recurrent chromosomal inversion implicates the homeobox gene Dlx5 in T-cell lymphomas from Lck-Akt2 transgenic mice. *Cancer Res* **68:** 1296 – 1302

Thoreen CC, Kang SA, Chang JW, Liu Q, Zhang J, Gao Y, Reichling LJ, Sim T, Sabatini DM, Gray NS (2009) An ATP-competitive mTOR inhibitor reveals rapamycin-insensitive functions of mTORC1. *J Biol Chem* **284:** 8023 – 8032

Topisirovic I, Ruiz-Gutierrez M, Borden KL (2004) Phosphorylation of the eukaryotic translation initiation factor eIF4E contributes to its transformation and mRNA transport activities. *Cancer Res* **64:** 8639 – 8642

Ueda T, Sasaki M, Elia AJ, Chio II, Hamada K, Fukunaga R, Mak TW (2010) Combined deficiency for MAP kinase-interacting kinase 1 and 2 (Mnk1 and Mnk2) delays tumor development. *Proc Natl Acad Sci USA* **107:** 13984 – 13990

von Manteuffel SR, Dennis PB, Pullen N, Gingras AC, Sonenberg N, Thomas G (1997) The insulin-induced signalling pathway leading to S6 and initiation factor 4E binding protein 1 phosphorylation bifurcates at a rapamycin-sensitive point immediately upstream of p70s6k. *Mol Cell Biol* **17:** 5426 – 5436

Wang R, Geng J, Wang JH, Chu XY, Geng HC, Chen LB (2009) Overexpression of eukaryotic initiation factor 4E (eIF4E) and its clinical significance in lung adenocarcinoma. *Lung Cancer* **66:** 237 – 244

Wang X, Li W, Williams M, Terada N, Alessi DR, Proud CG (2001) Regulation of elongation factor 2 kinase by p90(RSK1) and p70 S6 kinase. *EMBO J* **20:** 4370 – 4379

Westman B, Beeren L, Grudzien E, Stepinski J, Worch R, Zuberek J, Jemielity J, Stolarski R, Darzynkiewicz E, Rhoads RE, Preiss T (2005) The antiviral drug ribavirin does not mimic the 7-methylguanosine moiety of the mRNA cap structure *in vitro*. *RNA* **11:** 1505 – 1513

Yan Y, Svitkin Y, Lee JM, Bisaillon M, Pelletier J (2005) Ribavirin is not a functional mimic of the 7-methyl guanosine mRNA cap. *RNA* **11:** 1238 – 1244

Zhou BP, Liao Y, Xia W, Zou Y, Spohn B, Hung MC (2001) HER-2/neu induces p53 ubiquitination via Akt-mediated MDM2 phosphorylation. *Nat Cell Biol* **3:** 973 – 982